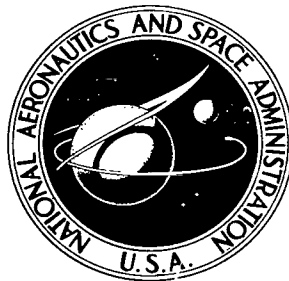


NASA TECHNICAL NOTE



NASA TN D-6312

C.1

NASA TN D-6312

LOAN COPY: RETURN  
AFWL (DOGL)  
KIRTLAND AFB, N

0133105



TECH LIBRARY KAFB, NM

NUMERICAL SOLUTION OF THE  
UNSTEADY NAVIER-STOKES EQUATIONS  
AND APPLICATION TO FLOW IN A  
RECTANGULAR CAVITY WITH A MOVING WALL

by *Leo F. Donovan*

*Lewis Research Center*

*Cleveland, Ohio 44135*



NATIONAL AERONAUTICS AND SPACE ADMINISTRATION • WASHINGTON, D.C. 20546 APRIL 1971



0133105

|   |  |   |
|---|--|---|
| 1. Report No.<br>NASA TN D-6312   | 2. Government Accession No.                            | 3. Receipt No.<br>0133105                               |
| 4. Title and Subtitle<br>NUMERICAL SOLUTION OF THE UNSTEADY<br>NAVIER-STOKES EQUATIONS AND APPLICATION TO FLOW IN<br>A RECTANGULAR CAVITY WITH A MOVING WALL  | 5. Report Date<br>April 1971                           | 6. Performing Organization Code                         |
| 7. Author(s)<br>Leo F. Donovan  | 8. Performing Organization Report No.<br>E-5577        | 10. Work Unit No.<br>129-01                             |
| 9. Performing Organization Name and Address<br>Lewis Research Center<br>National Aeronautics and Space Administration<br>Cleveland, Ohio 44135  | 11. Contract or Grant No.                              | 13. Type of Report and Period Covered<br>Technical Note |
| 12. Sponsoring Agency Name and Address<br>National Aeronautics and Space Administration<br>Washington, D.C. 20546   | 14. Sponsoring Agency Code                             |   |
| 15. Supplementary Notes   |  |   |
| 16. Abstract<br>A computer program to solve the two-dimensional, incompressible Navier-Stokes equations was written in FORTRAN IV. The program was used to investigate the startup of flow inside a cavity with the upper wall moving at constant velocity. Results are given for rectangular cavities with aspect ratios of 1/2 and 2 at a Reynolds number of 100 and for square cavities at Reynolds numbers between 100 and 500. The unsteady results at large times are compared where possible to velocities calculated from the steady Navier-Stokes equations and to the results of steady experiments; good agreement is shown. In addition, a numerical flow visualization technique is described and used to make a motion picture showing the results of the calculations. |  |   |
| 17. Key Words (Suggested by Author(s))<br>Numerical analysis<br>Computer program<br>Unsteady flow<br>Cavities<br>Numerical flow visualization<br>Motion pictures  | 18. Distribution Statement<br>Unclassified - unlimited |   |
| 19. Security Classif. (of this report)<br>Unclassified  | 20. Security Classif. (of this page)<br>Unclassified   | 21. No. of Pages<br>60                                  |
|   |  | 22. Price*<br>\$3.00                                    |



# CONTENTS

|  | Page |
|--|------|
| SUMMARY . . . . .  | 1    |
| INTRODUCTION . . . . .   | 1    |
| ANALYSIS . . . . .   | 2    |
| Differential Equations . . . . .                                 | 2    |
| Finite Difference Equations . . . . .                            | 4    |
| Computational mesh . . . . .                                     | 4    |
| Representation of derivatives . . . . .                          | 5    |
| Difference equations . . . . .                                   | 6    |
| Initial and Boundary Conditions . . . . .                        | 8    |
| No-slip wall . . . . .   | 8    |
| Impermeable wall . . . . .                                       | 9    |
| Pressure . . . . .   | 9    |
| Numerical Flow Visualization Experiment . . . . .                | 10   |
| CAVITY FLOW. . . . .   | 11   |
| Background . . . . .   | 11   |
| Remarks . . . . .  | 13   |
| Discussion of Results . . . . .                                  | 14   |
| Aspect ratio, 1/2; Reynolds number, 100 . . . . .                | 14   |
| Aspect ratio, 2; Reynolds number, 100 . . . . .                  | 16   |
| Square cavity . . . . .  | 19   |
| Flow visualization . . . . .                                     | 25   |
| CONCLUDING REMARKS . . . . .                                     | 31   |
| APPENDIXES   |      |
| A - SYMBOLS . . . . .  | 32   |
| B - DESCRIPTION OF COMPUTER PROGRAM . . . . .                    | 34   |
| C - OUTPUT FROM SAMPLE PROBLEM AT DIMENSIONLESS TIME 2 . . . . . | 37   |
| D - COMPUTER PROGRAM LISTING . . . . .                           | 39   |
| REFERENCES . . . . .   | 55   |

# NUMERICAL SOLUTION OF THE UNSTEADY NAVIER-STOKES EQUATIONS AND APPLICATION TO FLOW IN A RECTANGULAR CAVITY WITH A MOVING WALL

by Leo F. Donovan  
Lewis Research Center

## SUMMARY

A computer program to solve the unsteady, two-dimensional, incompressible Navier-Stokes equations was written in FORTRAN IV. The numerical method makes use of an iterative solution of a Poisson's equation for pressure followed by an explicit calculation of velocities. The computer program is included as an appendix.

Unsteady flow in a two-dimensional, rectangular cavity with the upper wall moving at constant velocity is investigated using the computer program. The calculations start with the fluid at rest in the cavity and continue until no further changes in velocity occur. Results for cavities with aspect ratios of  $1/2$ , 1, and 2 are presented for a Reynolds number of 100. For a square cavity, results are also given for several Reynolds numbers between 100 and 500. Velocities calculated from the unsteady Navier-Stokes equations at large times are compared where possible to velocities calculated from the steady Navier-Stokes equations and to the results of steady experiments; good agreement is shown.

A technique for conducting a numerical flow visualization experiment in conjunction with the solution of the Navier-Stokes equations is described. The results of the experiment are recorded on film which can be shown as a motion picture. Selected frames from the motion picture made during the investigation of cavity flow are reproduced in this report to illustrate this method of data presentation.

## INTRODUCTION

The availability of large, high-speed computers allows us to attack some formidable and interesting problems. One such area of research is in the solution of nonlinear partial differential equations describing physical phenomena. Analytic solutions can only be

obtained for certain special cases. In addition, the nonlinearity of the equations makes them much more difficult to solve numerically than linear equations. However, some progress has been made. The book by Ames (ref. 1) summarizes much of this work.

An additional difficulty with numerical solutions of partial differential equations is that they provide a mass of detailed information that is very hard to assimilate and understand. In order to overcome this problem Fromm and Harlow (ref. 2) have devised a visual display technique for presenting the results of their fluid dynamics calculations. This technique is analogous to a flow visualization experiment in the laboratory, in which a tracer is introduced into a fluid to make the flow visible.

Fluid motion is governed by the continuity equation and Navier-Stokes equations, expressing conservation of mass and momentum. Almost all the numerical solutions of these equations have been for two-dimensional flows. Some investigators have transformed the equations to stream function and vorticity coordinates. Pearson (ref. 3), for example, has treated rotating disks in this manner. Other investigators have chosen to retain velocity and position coordinates. Work by Harlow and coworkers (ref. 4) on free surface flows falls in this category. Since Harlow's method has the advantages of combining a successful numerical technique with visual display we have used it without the free-surface feature in our studies.

The results of a numerical investigation of incompressible flow in a square cavity at a Reynolds number of 100 are presented in reference 5. The present report describes an extension of the technique to rectangular cavities and higher Reynolds numbers. The differential equations describing unsteady, incompressible flow are discussed first. The corresponding difference equations are then derived and the numerical method used to solve them is presented. The method is then used to calculate the startup of flow in a rectangular cavity with a moving wall.

An advantage of the technique is that unsteady results are obtained. However, since no unsteady experimental results or prior calculation for cavity flow are available, only comparisons at steady conditions are possible. Results for rectangular cavities with aspect ratios of 1/2 and 2 are presented for a Reynolds number of 100. For flow in a square cavity, results are given for Reynolds numbers from 100 to 500.

## ANALYSIS

### Differential Equations

Conservation of mass and momentum are expressed by the continuity equation and Navier-Stokes equations, respectively. For constant density and viscosity the two-dimensional forms of these equations for a Newtonian fluid are (ref. 6)

$$\frac{\partial \bar{u}}{\partial \bar{x}} + \frac{\partial \bar{v}}{\partial \bar{y}} = 0 \quad (1)$$

$$\frac{\partial \bar{u}}{\partial t} + \bar{u} \frac{\partial \bar{u}}{\partial \bar{x}} + \bar{v} \frac{\partial \bar{u}}{\partial \bar{y}} = - \frac{1}{\bar{\rho}} \frac{\partial \bar{P}}{\partial \bar{x}} + \bar{\nu} \left( \frac{\partial^2 \bar{u}}{\partial \bar{x}^2} + \frac{\partial^2 \bar{u}}{\partial \bar{y}^2} \right) + \bar{g}_x \quad (2)$$

$$\frac{\partial \bar{v}}{\partial t} + \bar{u} \frac{\partial \bar{v}}{\partial \bar{x}} + \bar{v} \frac{\partial \bar{v}}{\partial \bar{y}} = - \frac{1}{\bar{\rho}} \frac{\partial \bar{P}}{\partial \bar{y}} + \bar{\nu} \left( \frac{\partial^2 \bar{v}}{\partial \bar{x}^2} + \frac{\partial^2 \bar{v}}{\partial \bar{y}^2} \right) + \bar{g}_y \quad (3)$$

In these equations  $\bar{u}$  and  $\bar{v}$  are the velocity components in the  $\bar{x}$  and  $\bar{y}$  directions,  $\bar{P}$  is the pressure, and  $\bar{g}_x$  and  $\bar{g}_y$  are the body forces in the  $\bar{x}$  and  $\bar{y}$  directions. The overbars are used to denote dimensional quantities.

The equations can be made dimensionless with a reference velocity  $\bar{W}$ , a reference length  $\bar{L}$ , and the fluid viscosity  $\bar{\nu}$  by the following substitutions:

$$\left. \begin{aligned} u &= \frac{\bar{u}}{\bar{W}} & v &= \frac{\bar{v}}{\bar{W}} \\ x &= \frac{\bar{x}}{\bar{L}} & y &= \frac{\bar{y}}{\bar{L}} \\ t &= \frac{\bar{W}t}{\bar{L}} & \varphi &= \frac{\bar{P}}{\bar{\rho}\bar{W}^2} \\ \nu &= \frac{\bar{\nu}}{\bar{L}\bar{W}} \\ g_x &= \frac{\bar{L}g_x}{\bar{W}^2} & g_y &= \frac{\bar{L}g_y}{\bar{W}^2} \end{aligned} \right\} \quad (4)$$

The viscosity  $\nu$  is thus the reciprocal of the Reynolds number.

The dimensionless forms of equations (1) to (3) then become

$$\frac{\partial u}{\partial x} + \frac{\partial v}{\partial y} = 0 \quad (5)$$

$$\frac{\partial u}{\partial t} + u \frac{\partial u}{\partial x} + v \frac{\partial u}{\partial y} = - \frac{\partial \varphi}{\partial x} + \nu \left( \frac{\partial^2 u}{\partial x^2} + \frac{\partial^2 u}{\partial y^2} \right) + g_x \quad (6)$$

$$\frac{\partial v}{\partial t} + u \frac{\partial v}{\partial x} + v \frac{\partial v}{\partial y} = - \frac{\partial \varphi}{\partial y} + \nu \left( \frac{\partial^2 v}{\partial x^2} + \frac{\partial^2 v}{\partial y^2} \right) + g_y \quad (7)$$

The continuity equation can be used to write equations (6) and (7) in forms such that the resulting finite difference equations will rigorously conserve momentum (see ref. 4). Thus

$$\frac{\partial u}{\partial t} + \frac{\partial u^2}{\partial x} + \frac{\partial uv}{\partial y} = - \frac{\partial \varphi}{\partial x} + \nu \left( \frac{\partial^2 u}{\partial y^2} - \frac{\partial^2 v}{\partial x \partial y} \right) + g_x \quad (8)$$

$$\frac{\partial v}{\partial t} + \frac{\partial v^2}{\partial y} + \frac{\partial uv}{\partial x} = - \frac{\partial \varphi}{\partial y} + \nu \left( \frac{\partial^2 v}{\partial x^2} - \frac{\partial^2 u}{\partial x \partial y} \right) + g_y \quad (9)$$

If the x- and y-momentum equations are differentiated with respect to x and y, respectively, and the results are added and rearranged, the following Poisson's equation for pressure is obtained

$$\frac{\partial^2 \varphi}{\partial x^2} + \frac{\partial^2 \varphi}{\partial y^2} = - \frac{\partial}{\partial t} \left( \frac{\partial u}{\partial x} + \frac{\partial v}{\partial y} \right) - \frac{\partial^2 u^2}{\partial x^2} - 2 \frac{\partial^2 uv}{\partial x \partial y} - \frac{\partial^2 v^2}{\partial y^2} \quad (10)$$

The first term to the right of the equality sign in this equation is the time derivative of the left side of the continuity equation and, as such, should be zero. However, since the continuity equation will not be satisfied exactly, this term is retained as a correction.

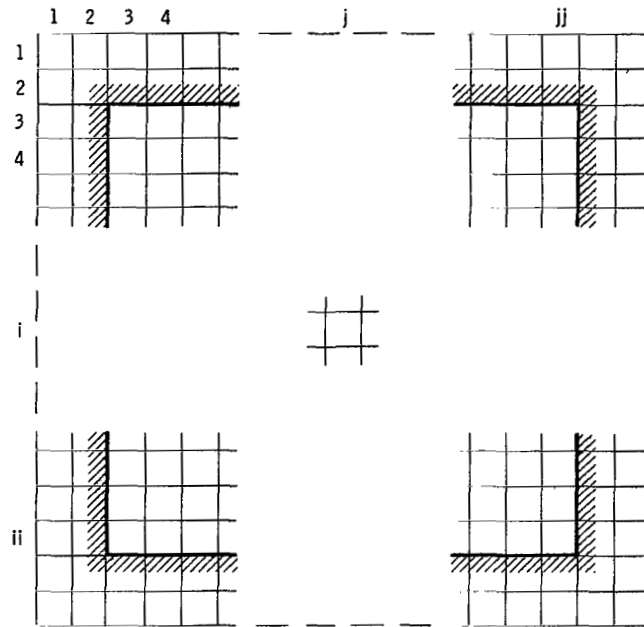
## Finite Difference Equations

Computational mesh. - The finite difference mesh is shown in figure 1. The positions of the variables are chosen so that vertical walls pass through positions where the u-component of velocity is defined, horizontal walls pass through positions where the v-component of velocity is defined, and pressures are cell-centered. These positions have been chosen to facilitate application of the boundary conditions.

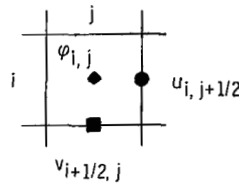
If it is necessary to evaluate one of the variables at a position where it is not defined, an average is used. For example,

$$u_{i,j} = \frac{1}{2} (u_{i,j+1/2} + u_{i,j-1/2}) \quad (11)$$





(A) ENTIRE MESH.



(B) TYPICAL CELL.

Figure 1. - Computational mesh.

For conciseness, however, terms such as  $u_{i,j}$  will be retained in the equations throughout the remainder of this section.

Representation of derivatives. - When converting the differential equations to finite difference form, centered differences are used to represent derivatives. For example,  $\partial u / \partial x$  and  $\partial^2 u / \partial x^2$  are approximated at the point  $(i,j)$  by

$$\frac{1}{\delta x} (u_{i,j+1/2} - u_{i,j-1/2})$$

and

$$\frac{1}{\delta x^2} (u_{i,j+1} - 2u_{i,j} + u_{i,j-1})$$

When the derivative of a product of undefined quantities is formed, the product is differentiated and then averages are formed. For example,  $\partial^2(uv)/\partial x \partial y$  at the point  $(i, j)$  is replaced by

$$\frac{1}{\delta x \delta y} \left[ (uv)_{i+1/2, j+1/2} - (uv)_{i-1/2, j+1/2} - (uv)_{i+1/2, j-1/2} + (uv)_{i-1/2, j-1/2} \right]$$

A typical average is then

$$(uv)_{i+1/2, j+1/2} = \frac{1}{4} (u_{i+1, j+1/2} + u_{i, j+1/2})(v_{i+1/2, j+1} + v_{i+1/2, j}) \quad (12)$$

Difference equations. - If the abbreviation

$$d_{i,j} = \frac{1}{\delta x} (u_{i, j+1/2} - u_{i, j-1/2}) + \frac{1}{\delta y} (v_{i+1/2, j} - v_{i-1/2, j}) \quad (13)$$

is introduced, the finite difference form of the continuity equation can be written as

$$d_{i,j} = 0 \quad (14)$$

Formally, the time derivative of the continuity equation is then

$$\frac{1}{\delta t} (d_{i,j}^{n+1} - d_{i,j}^n) = 0 \quad (15)$$

where the superscripts  $n+1$  and  $n$  refer to the advanced time and the current time, respectively. Hereinafter, the lack of a superscript will indicate the current time.

The finite difference Poisson's equation for pressure can be obtained from equation (10)

$$\varphi_{i,j} = \frac{1}{2 \left( \frac{1}{\delta x^2} + \frac{1}{\delta y^2} \right)} \left( \frac{\varphi_{i, j+1} + \varphi_{i, j-1}}{\delta x^2} + \frac{\varphi_{i+1, j} + \varphi_{i-1, j}}{\delta y^2} + r_{i,j} \right) \quad (16)$$

where

$$\begin{aligned}
r_{i,j} = & \frac{1}{\delta x^2} (u_{i,j+1}^2 - 2u_{i,j}^2 + u_{i,j-1}^2) \\
& + \frac{2}{\delta x \delta y} [ (uv)_{i+1/2,j+1/2} - (uv)_{i-1/2,j+1/2} - (uv)_{i+1/2,j-1/2} + (uv)_{i-1/2,j-1/2} ] \\
& + \frac{1}{\delta y^2} (v_{i+1,j}^2 - 2v_{i,j}^2 + v_{i-1,j}^2) - \frac{1}{\delta t} d_{i,j}
\end{aligned} \tag{17}$$

The final term arises because equation (16) will be solved iteratively and therefore the continuity equation will not be satisfied exactly. The discrepancy  $d_{i,j}^n$  from the current time is used as a correction during the calculations at the advanced time. Since it is desired that the continuity equation be satisfied as closely as possible at the advanced time, the  $d_{i,j}^{n+1}$  are set to zero. If the correction terms were not included in equation (16), the pressure iteration would have to be carried further; this would require more computer time than the technique used here. Hirt and Harlow (ref. 7) discuss the use of a correction term in more detail.

The finite difference forms of equations (2) and (3) for the velocities are

$$\begin{aligned}
u_{i,j+1/2}^{n+1} = & u_{i,j+1/2} + \delta t \left\{ -\frac{1}{\delta x} (u_{i,j+1}^2 - u_{i,j}^2) - \frac{1}{\delta y} [ (uv)_{i+1/2,j+1/2} - (uv)_{i-1/2,j+1/2} ] \right. \\
& - \frac{1}{\delta x} (\varphi_{i,j+1} - \varphi_{i,j}) + \nu \left[ \frac{1}{\delta y^2} (u_{i+1,j+1/2} - 2u_{i,j+1/2} + u_{i-1,j+1/2}) \right. \\
& \left. \left. - \frac{1}{\delta x \delta y} (v_{i+1/2,j+1} - v_{i+1/2,j} - v_{i-1/2,j+1} + v_{i-1/2,j}) \right] + g_x \right\}
\end{aligned} \tag{18}$$

$$\begin{aligned}
v_{i+1/2,j}^{n+1} = v_{i+1/2,j} + \delta t \left\{ -\frac{1}{\delta x} \left[ (uv)_{i+1/2,j+1/2} - (uv)_{i+1/2,j-1/2} \right] \right. \\
- \frac{1}{\delta y} (v_{i+1,j}^2 - v_{i,j}^2) - \frac{1}{\delta y} (\varphi_{i+1,j} - \varphi_{i,j}) \\
+ \nu \left[ \frac{1}{\delta x^2} (v_{i+1/2,j+1} - 2v_{i+1/2,j} + v_{i+1/2,j-1}) \right. \\
\left. \left. - \frac{1}{\delta x \delta y} (u_{i+1,j+1/2} - u_{i,j+1/2} - u_{i+1,j-1/2} + u_{i,j-1/2}) \right] + g_y \right\} \quad (19)
\end{aligned}$$

These two equations are solved at each time step after the pressure has been determined.

## Initial and Boundary Conditions

The specific problem to be solved will determine the initial and boundary conditions. At a no-slip wall the tangential component of velocity is equal to the wall velocity; if the wall is impermeable, the normal component of velocity is zero. At slip walls (i. e., planes of symmetry) the normal component of velocity is zero and the normal gradient of the tangential component is zero. If fluid is entering and leaving the computing region, sufficient information must be provided at the inlet and outlet to make the problem determinant. If the fluid starts from rest, the initial conditions are simply that the velocities are everywhere zero and the pressure is uniform.

For cavity flow, which is discussed later in this report, the appropriate boundary conditions are no-slip, impermeable walls. One of the walls is moving at constant velocity and the other three walls are stationary.

No-slip wall. - Fictitious tangential velocities outside the cavity are defined because they are needed when equations (16) to (19) are solved for the row of cells just inside the cavity. These fictitious tangential velocities are defined so that the interpolated values of velocity at the wall satisfy the no-slip boundary condition. The fictitious velocities are calculated at each time step, after the velocities inside the cavity have been evaluated.

For a vertical wall at  $j - (1/2)$ , figure 2(a), the fictitious velocity  $v_{i-1/2,j-1}$  would be evaluated so that

$$v_{i-1/2, j-1/2} = \frac{1}{2} (v_{i-1/2, j-1} + v_{i-1/2, j}) = \text{Constant} \quad \text{all } i \quad (20)$$

where the constant is the wall velocity, which is zero for a stationary wall or unity for the moving wall.

Similarly, for a horizontal wall at  $i - (1/2)$ , figure 2(b), the fictitious velocity  $u_{i-1, j-1/2}$  would be evaluated so that

$$u_{i-1/2, j-1/2} = \frac{1}{2} (u_{i-1, j-1/2} + u_{i, j-1/2}) = \text{Constant} \quad \text{all } j \quad (21)$$

where the constant is again the wall velocity.

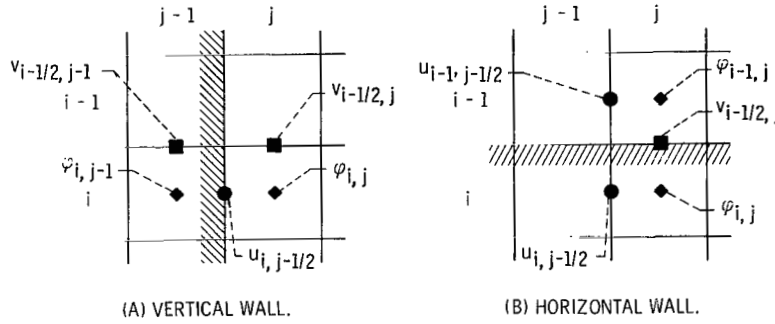


Figure 2. - Boundary conditions.

Impermeable wall. - The normal velocity at an impermeable wall can be written directly. For a vertical wall at  $j - (1/2)$ , figure 2(a),

$$u_{i, j-1/2} = 0 \quad \text{all } i \quad (22)$$

For a horizontal wall at  $i - (1/2)$ , figure 2(b),

$$v_{i-1/2, j} = 0 \quad \text{all } j \quad (23)$$

Pressure. - Fictitious pressures outside the cavity are also defined because they are needed in the solution of equation (16) for the row of cells just inside the cavity. The Navier-Stokes equations can be evaluated at the walls to determine the fictitious pressures since the normal component of velocity is always zero at an impermeable wall. For a left stationary wall at  $j - (1/2)$ , figure 2(a), the fictitious pressure  $\varphi_{i, j-1}$  can be calculated from equation (18) as

$$\varphi_{i,j-1} = \varphi_{i,j} + \frac{2\nu}{\delta y} (v_{i+1/2,j} - v_{i-1/2,j}) \quad (24)$$

For a stationary bottom wall at  $i = (1/2)$ , figure 2(b), the fictitious pressure  $\varphi_{i,j}$  can be calculated from equation (19) as

$$\varphi_{i,j} = \varphi_{i-1,j} + \frac{2\nu}{\delta x} (u_{i-1,j+1/2} - u_{i-1,j-1/2}) \quad (25)$$

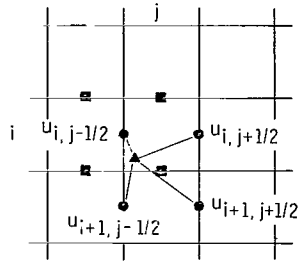
The velocities are known, either from the initial condition or the previous time cycle.

## Numerical Flow Visualization Experiment

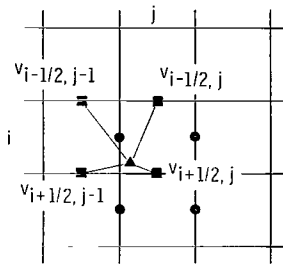
The traditional way of presenting the results of experimental or numerical fluid mechanical investigations is not the best way of helping one form a coherent, overall picture of a complicated flow situation, especially if the flow is unsteady. Flow visualization experiments, in which a tracer is introduced into the fluid to make its movement visible, have been designed to overcome this difficulty in the laboratory. A numerical analog of a laboratory flow visualization experiment offers the same advantages for numerical fluid dynamics studies. The technique devised by Fromm and Harlow (ref. 2) employs special marked particles that move with the fluid as the tracer. A microfilm recorder is used to photograph the marked particles displayed on a cathode ray tube. The sequence of photographs, when viewed as a motion picture, shows the behavior of the fluid clearly. The marked particles serve only to make the flow visible and do not enter into the solution of the Navier-Stokes equations.

The flow visualization experiment is conducted as follows: At the start of the calculation an initial uniform distribution of either one or four particles per cell is imagined to be distributed throughout the fluid. Particles at these positions are displayed as small plus signs on the cathode ray tube and are then photographed. Thereafter, at each time step in the calculation, the particles are moved with velocities appropriate to their location and time, displayed on the cathode ray tube, and photographed.

The distance a particle is moved is simply the product of the velocity at its current location and the time interval over which that velocity is assumed to exist (i. e., the time step in the solution of the Navier-Stokes equations). Since the particles will not in general be located precisely at positions where the velocities are known from the solution of the Navier-Stokes equations, a way of estimating their velocities is needed. The components of the velocity of a particle are calculated as the weighted averages of the velocities at the four closest positions at which those velocities are defined. Since  $u$  and  $v$  velocities are defined at different positions, velocities at eight positions will be involved in the movement of one particle. The weight assigned to a velocity is inversely propor-



(A) VELOCITY COMPONENT  $u$ .



(B) VELOCITY COMPONENT  $v$ .

Figure 3. - Calculation of particle velocity.

tional to its distance from the particle in question. Figure 3 shows a typical particle and the velocities that are used to estimate the particle velocity.

A film (C-271) entitled "Computer-Generated Flow-Visualization Motion Pictures" shows how this technique is used. A request card and a description of the film are included at the back of this report.

## CAVITY FLOW

### Background

As a specific example of a problem that can be solved with the technique presented in this report, consider the startup of flow in a long groove, over which an endless belt is drawn at constant velocity. A cutaway view of such a groove is shown in figure 4. This situation, which is difficult to study experimentally without disturbing the flow, has relevance in bearing and seal studies, where it is the limiting case of a spiral groove seal. In this case, the results of interest would be the integrated pressure over the belt, which is the net lift, and the minimum pressure, which would indicate whether cavitation would be a problem.

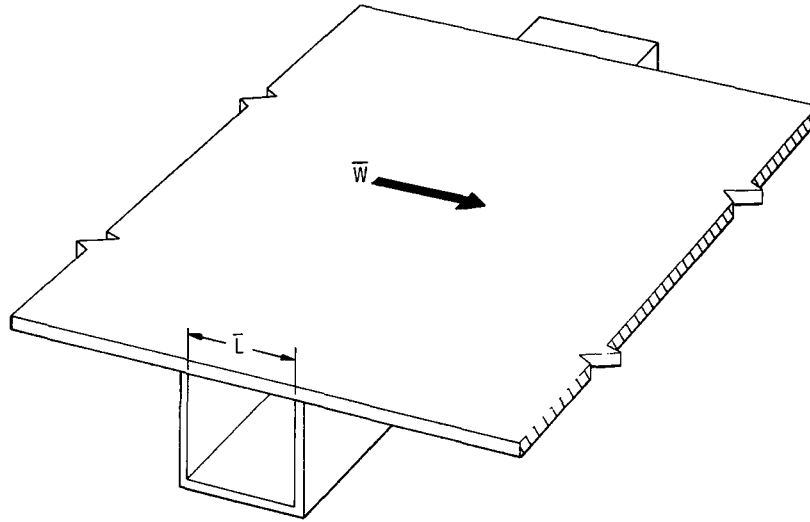


Figure 4. - Cutaway view of groove and belt.

If the groove is long enough, the flow at each cross section, except near an end, will be the same. Steady flows such as this have been investigated experimentally and numerically so that comparison with prior work is possible.

If the upper surface of a fluid-filled cavity is moving in its own plane with constant velocity, a circulatory motion of the fluid is set up within the cavity. Time-exposure photographs have been taken (refs. 8 and 9) of flows into which a tracer has been injected so that the qualitative features of the steady flow are known. For cavities with aspect ratios (i.e., depth/width) of 1 or less, most of the fluid rotates about a point - the vortex center - where the vector velocity is zero. The main vortex occupies most of the cavity but small, weak, counterrotating vortices exist in both lower corners. For a cavity with an aspect ratio of 2, there is, in addition, a large, weak, counterrotating vortex occupying most of the lower portion of the cavity.

Steady flow in a two-dimensional cavity has been analyzed (refs. 8 and 10 to 15) by numerically solving the steady Navier-Stokes equations. Burggraf (ref. 12) has also obtained an analytic solution to the linearized problem for an eddy bounded by a circular streamline. The starting flow problem, the fluid being initially at rest, was considered by Greenspan (ref. 16); however, only steady results were presented.

The technique devised by Harlow (ref. 4) for calculating free surface flows was used in reference 5 to solve the problem of unsteady flow in a square cavity at a Reynolds number of 100. The calculations were carried out until velocities were no longer changing, at which point they were in excellent agreement with a numerical solution of the steady Navier-Stokes equations. In addition, the terminal position of the unsteady vortex center agreed well with the position of a vortex center estimated from a time-exposure photograph of a steady vortex.



The parameters of interest are the aspect ratio of the cavity and the Reynolds number of the flow. Cavities with aspect ratios of  $1/2$ , 1, and 2 are studied at a Reynolds number of 100. Flows with Reynolds numbers between 100 and 500 are investigated in a square cavity.

## Remarks

For cavity flow it is convenient to choose the length and velocity of the moving wall as the reference length and velocity used to make the Navier-Stokes equations dimensionless. The cavity is assumed to be bounded by no-slip, impermeable walls. The fluid is at rest at the start of the calculation and the value for the initial uniform pressure is chosen to be unity. The reference location for pressure, where a value of unity is maintained, is the center of the wall opposite the moving wall.

Space increments of 0.05 and a time step of 0.02 were found to be satisfactory for Reynolds numbers from 100 to 500. Some of the calculations were also performed with space and time increments halved, and essentially the same results were obtained. Approximate stability criteria are discussed in appendix B.

A difficulty with particle movement arose when a particle was near a wall where the boundary layer was very thin. It was noticed that particles tended to congregate along the upper part of the right wall. Then a crescent-shaped region devoid of particles formed along most of the remaining part of the right wall and extended into the cavity. In order to circumvent this problem the calculation of tangential velocity components of particles within half a mesh spacing of a wall was modified.

A possible velocity profile in a thin boundary layer is marked "actual" in figure 5. If a particle is located at position P, for example, the interpolation scheme for particle movement using four mesh-point velocities underestimates particle velocity. If only the two mesh-point velocities within the cavity are used, particle velocity is overestimated. For the profiles shown in figure 5, however, the two-point interpolation is superior. This two-point interpolation scheme was used for particles within half a mesh spacing of a wall, and no further anomalous particle motion was noted.

About  $1/2$  minute of IBM System/360 Model 67 computer time was required per dimensionless time regardless of Reynolds number for a square cavity. However, longer runs were necessary to reach steady conditions at larger Reynolds numbers. The criterion of steady conditions we have used is that the position of the vortex center change less than 1 percent over a period of 5 dimensionless time units. For a Reynolds number of 100 this occurred at about a dimensionless time of 10; for a Reynolds number of 500, it was not reached until about a dimensionless time of 25. For cavities of aspect ratio  $1/2$  or 2, the number of mesh points in the longer direction was doubled and about twice as long a running time as for the square cavity was needed.

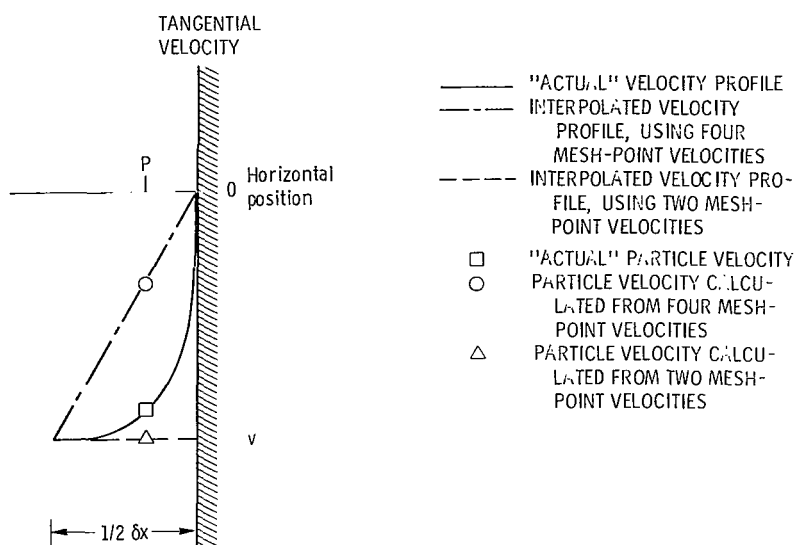


Figure 5. - Calculation of particle velocity in a thin boundary layer on a wall.

## Discussion of Results

Cavity flow is characterized by the aspect ratio and the Reynolds number. Aspect ratio is the cavity depth divided by the cavity width. Reynolds number is the product of the length and velocity of the moving wall divided by the fluid viscosity.

Aspect ratio, 1/2; Reynolds number, 100. - Figure 6 is a time-exposure photograph (ref. 8) of a steady vortex in a cavity with aspect ratio of 1/2 at a Reynolds number of 100. Washing powder has been added to oil to make the flow visible. A tape is pulled across the cavity to provide the moving surface. Figure 7 compares the position of the vortex center estimated from this photograph with the position calculated by Zuk and Renkel (ref. 15) from the steady Navier-Stokes equations and with the position determined from the unsteady Navier-Stokes equations at large time. The numerical solutions are in good agreement with the experimental value. The path of the instantaneous position of the vortex center is also shown; it starts under the midpoint of the moving wall, shifts downstream (i. e., in the direction of movement of the wall) and into the cavity, and turns upstream slightly to attain its terminal position.

Figures 8 and 9 compare terminal velocities from the solution of the unsteady Navier-Stokes equations with velocities calculated from the steady Navier-Stokes equations (ref. 15). The comparisons are shown as velocity traverses through the vortex center; figure 8 shows velocity parallel to the moving wall in the vertical traverse and figure 9 shows velocity perpendicular to the moving wall in the horizontal traverse. In both figures the agreement is good.

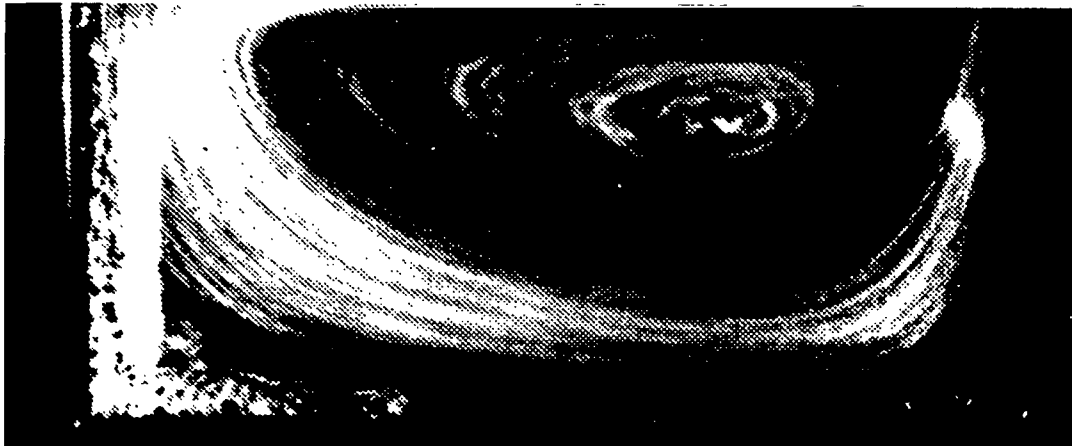


Figure 6. - Time-exposure photograph of vortex in cavity of aspect ratio 1/2. Reynolds number, 100. (From ref. 8.)

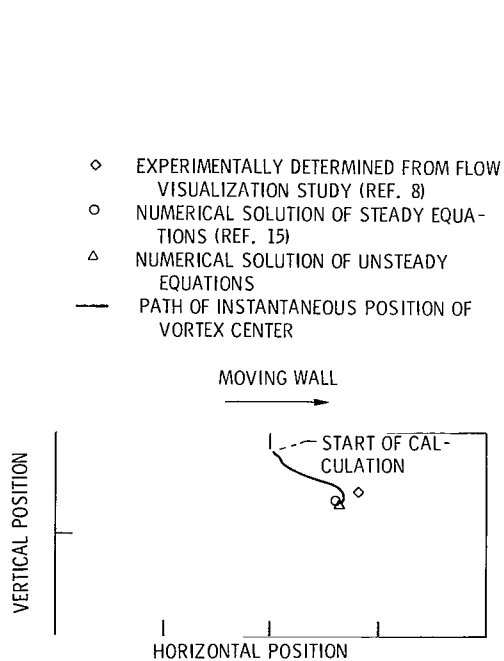


Figure 7. - Position of vortex center in cavity of aspect ratio 1/2. Reynolds number, 100.

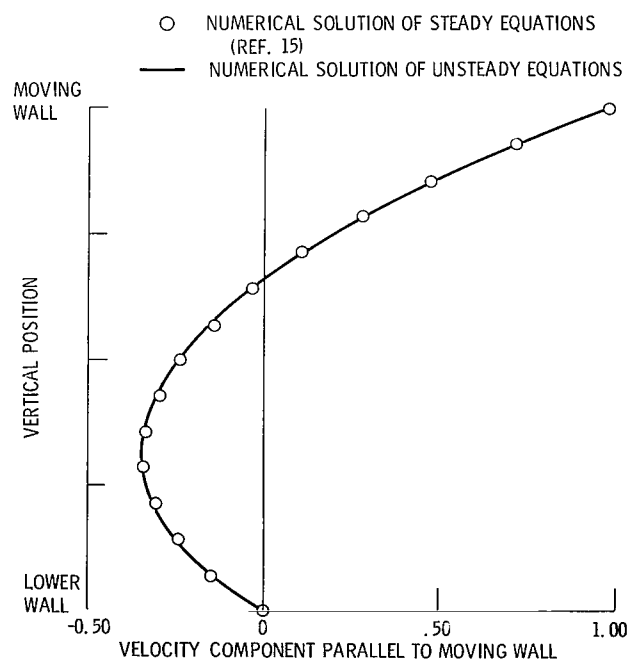


Figure 8. - Vertical velocity traverse through vortex center in cavity of aspect ratio 1/2. Reynolds number, 100.

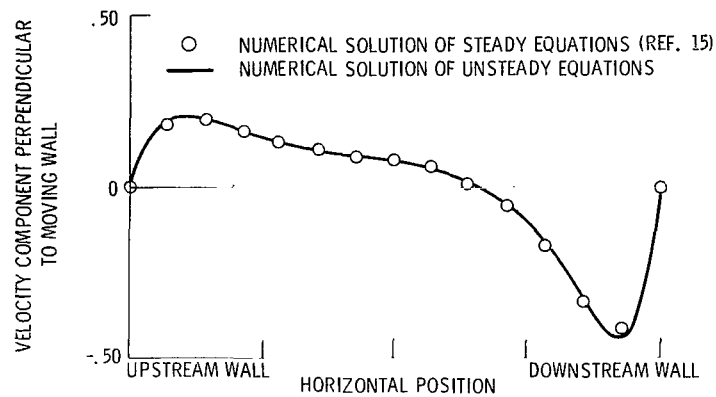


Figure 9. - Horizontal velocity traverse through vortex center in cavity of aspect ratio 1/2. Reynolds number, 100.

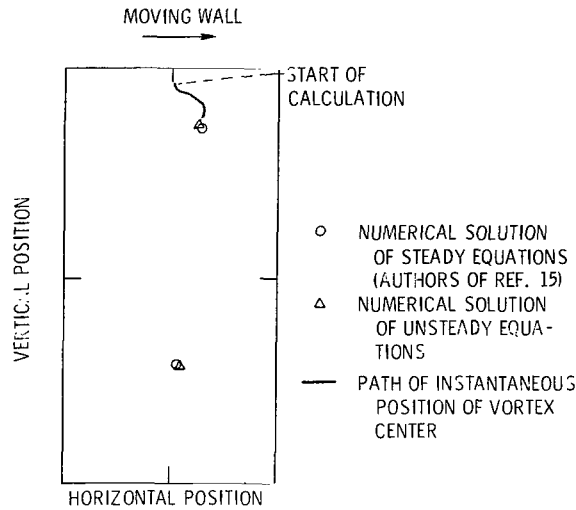


Figure 10. - Position of vortex centers in cavity of aspect ratio 2. Reynolds number, 100.

Aspect ratio, 2; Reynolds number, 100. - Two large vortices exist when the aspect ratio of the cavity is 2. Figure 10 compares the terminal positions of vortex centers calculated from solutions of the steady and unsteady Navier-Stokes equations at large times for a Reynolds number of 100. The authors of reference 15 calculated the steady case for comparison with the unsteady result. The numerical solutions are in good agreement with each other; no experimental value is available for comparison. The path of the instantaneous position of the upper vortex center is also shown and is similar to the path for cavities with aspect ratios of 1/2.

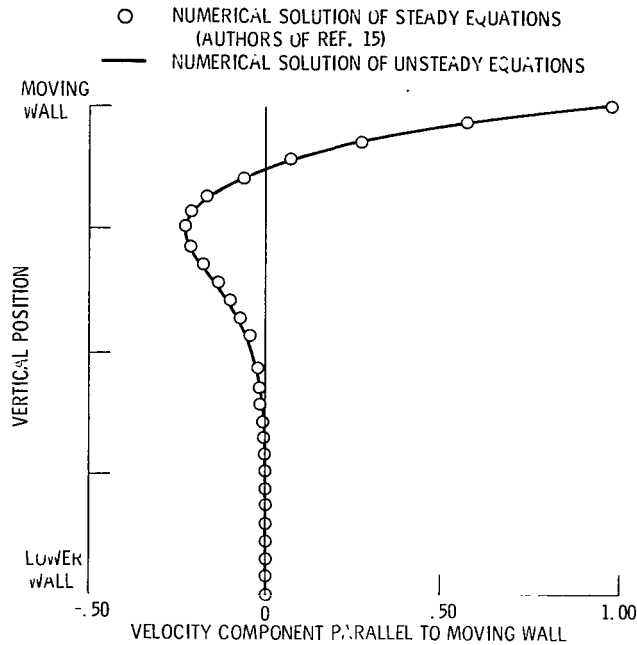


Figure 11. - Vertical velocity traverse through upper vortex center in cavity of aspect ratio 2. Reynolds number, 100.

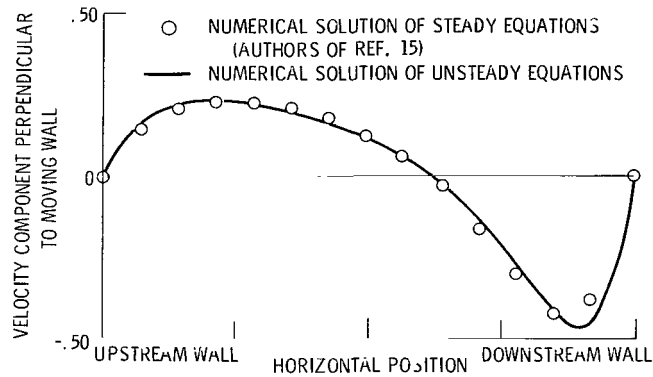
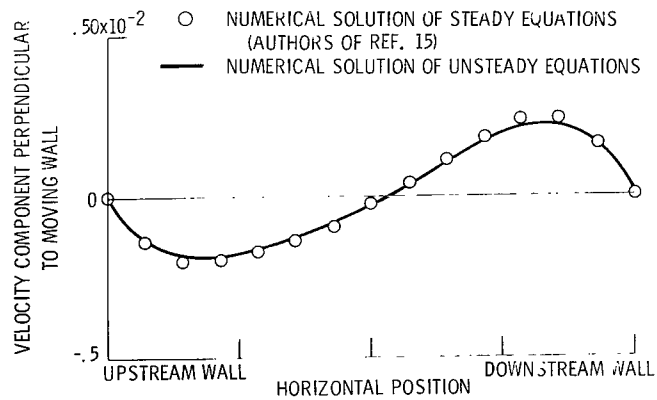
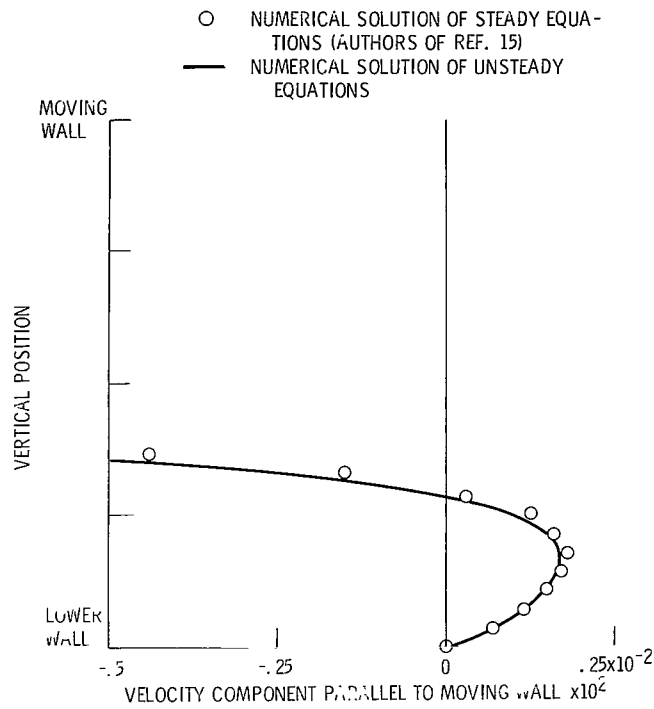


Figure 12. - Horizontal velocity traverse through upper vortex center in cavity of aspect ratio 2. Reynolds number, 100.

Figures 11 to 14 compare traverses of terminal velocities calculated from the unsteady Navier-Stokes equations with velocities calculated from the steady Navier-Stokes equations. The agreement between the solutions is good. Figures 11 and 12 are traverses through the upper vortex center. It can be seen that the flow in the upper part of the cavity is similar to the flow in the cavity with an aspect ratio of 1/2 shown in figures 8 and 9. Figures 13 and 14 are traverses through the lower vortex center. The flow in the lower part of the cavity is much slower (about two orders of magnitude) than in the upper part.



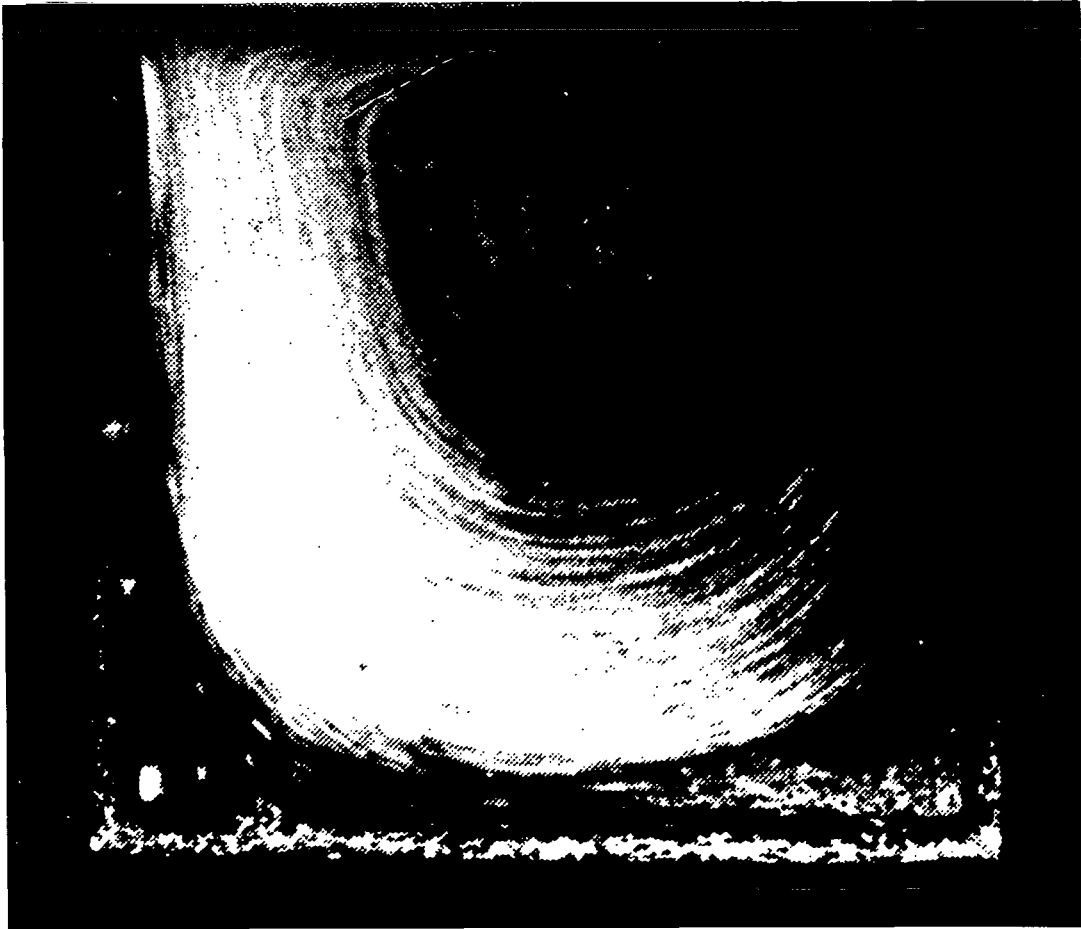


Figure 15. - Time-exposure photograph of vortex in square cavity. Reynolds number, 100. (From ref. 8.)

Square cavity. - Figure 15 is a time-exposure photograph (ref. 8) of a steady vortex in a square cavity at a Reynolds number of 100 from which the position of the vortex center can be estimated. Figure 16 compares this estimate with the positions determined from two numerical solutions of the steady Navier-Stokes equations (refs. 12 and 15) and the unsteady Navier-Stokes equations at large times. The agreement among these various methods is excellent. The path of the instantaneous position of the vortex center is also shown; it is similar to the paths for cavities with aspect ratios of  $1/2$  and  $2$ .

Figures 17 and 18 compare terminal velocities from the solution of the unsteady Navier-Stokes equations with velocities calculated from the steady Navier-Stokes equations (ref. 15). The curves, showing traverses through the vortex center, are similar to those already presented for a cavity with an aspect ratio of  $1/2$ . The agreement between the solutions is excellent. The flow in this square cavity is similar to the flows

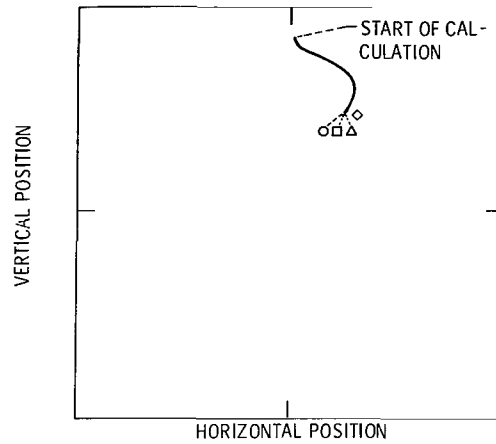
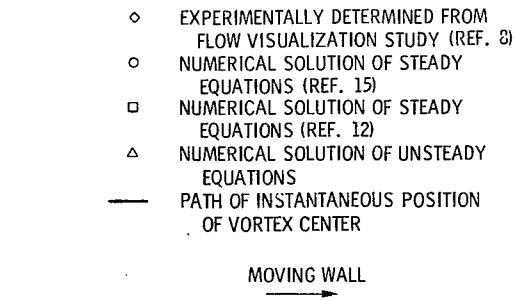


Figure 16. - Position of vortex center in square cavity. Reynolds number, 100.

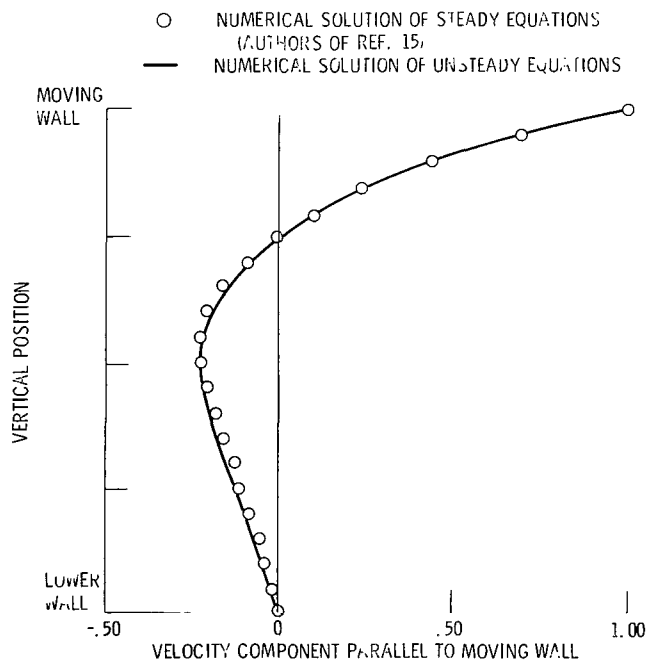


Figure 17. - Vertical velocity traverse through vortex center in square cavity. Reynolds number, 100.



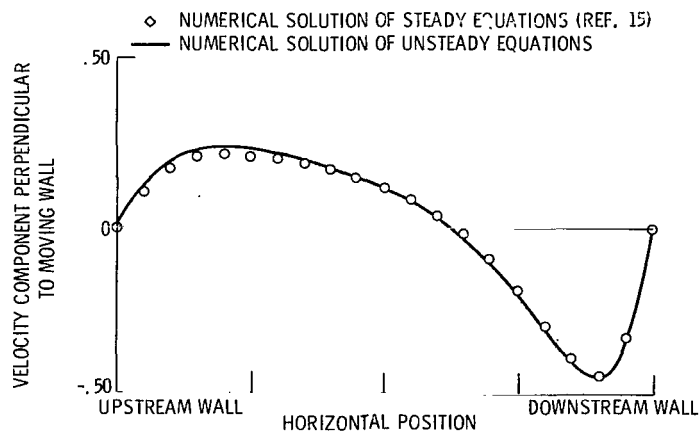


Figure 18. - Horizontal velocity traverse through vortex center in square cavity. Reynolds number, 100.

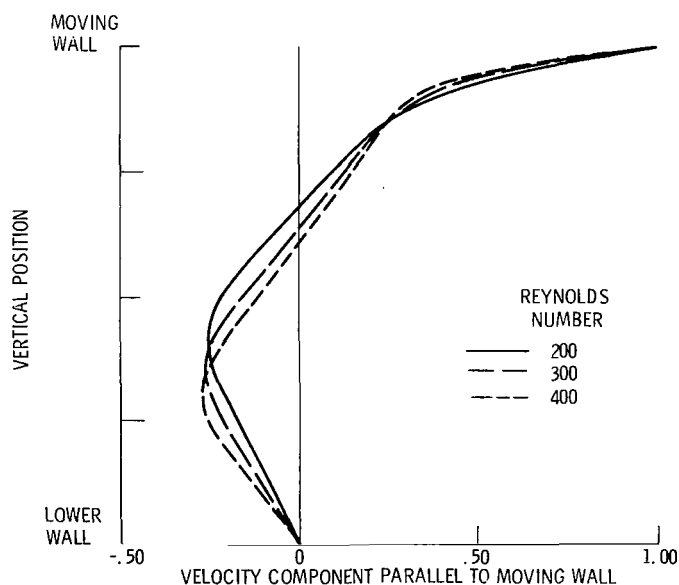


Figure 19. - Vertical velocity traverse through vortex center in square cavity.

in the cavity with an aspect ratio of  $1/2$  and the upper part of the cavity with an aspect ratio of 2.

Figures 19 and 20 show how velocity traverses through the vortex center change as Reynolds number is increased from 200 to 400 in a square cavity. For larger Reynolds numbers the extent of the inviscid portion of the flow is greater. This is shown by the increased portion of the velocity profile that is linear about the vortex center. The only prior calculation available for comparison (ref. 12), a vertical traverse from a solution

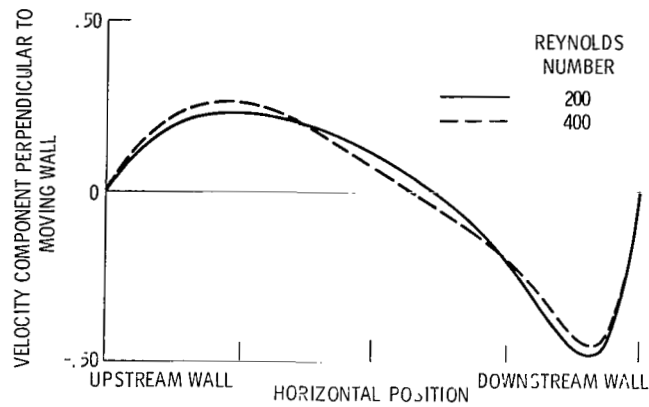


Figure 20. - Horizontal velocity traverse through vortex center in square cavity.

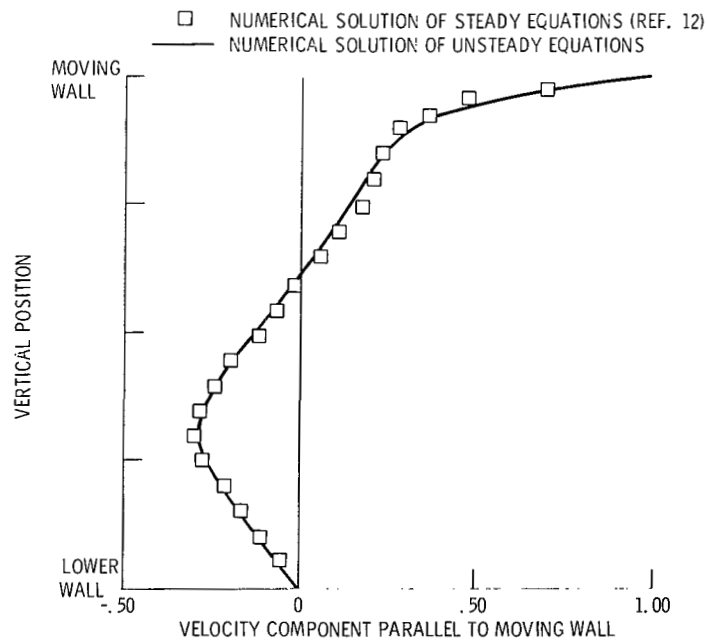


Figure 21. - Vertical velocity traverse through vortex center in square cavity. Reynolds number, 400.

of the steady Navier-Stokes equations at a Reynolds number of 400, shows good agreement in figure 21 with the solution of the unsteady Navier-Stokes equations at large times.

Figures 22 and 23 show velocity traverses through the vortex center in a square cavity for a Reynolds number of 500 at various times. It can be seen that at successively larger times the inviscid portion of the flow occupies progressively larger fractions of the cavity.

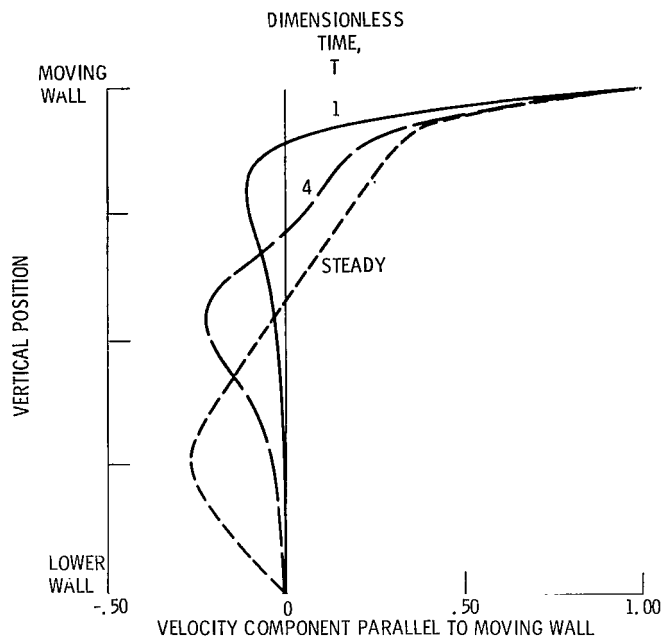


Figure 22. - Vertical velocity traverses through vortex centers in square cavity. Reynolds number, 500.

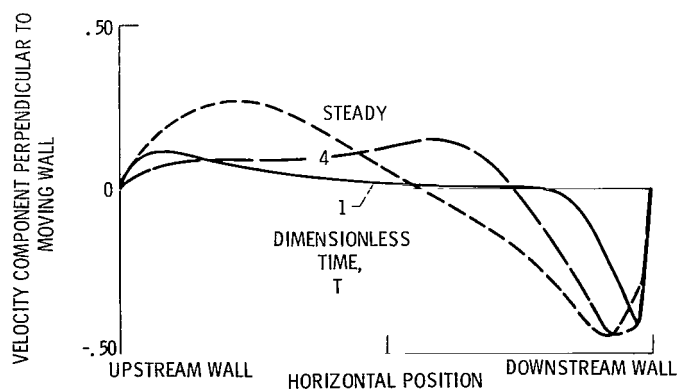
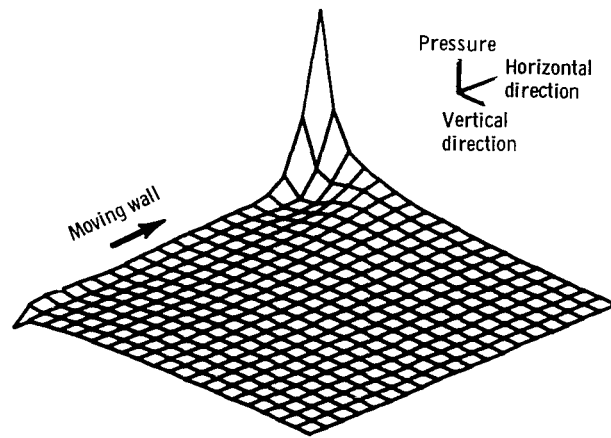
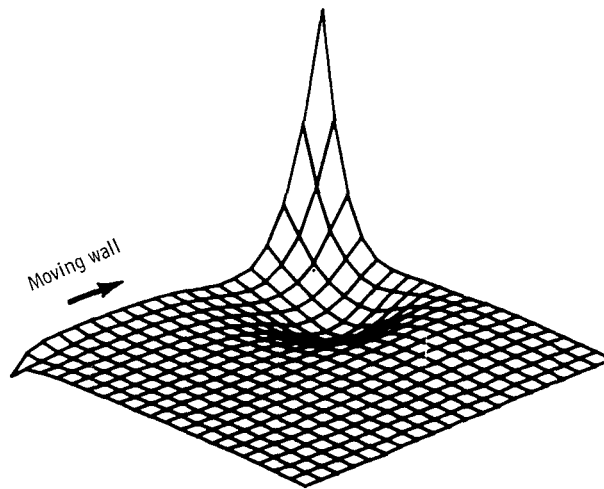


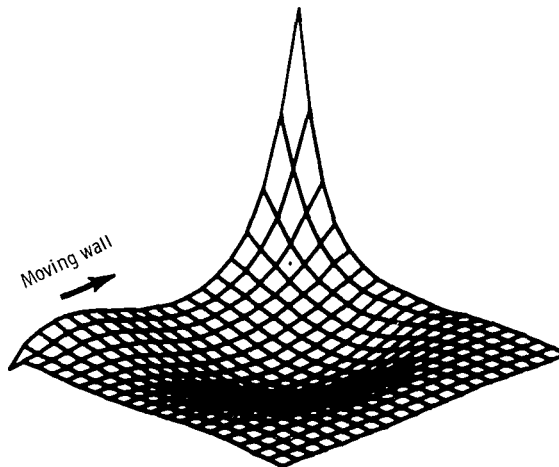
Figure 23. - Horizontal velocity traverses through vortex centers in square cavity. Reynolds number, 500.



(a) Time, 1.



(b) Time, 4.



(c) Steady.

Figure 24. - Pressure distribution in square cavity. Reynolds number, 500.  
Dimensionless time.

Figure 24 shows three-dimensional plots of the pressure fields for a Reynolds number of 500 and the same times as the velocity traverses shown in figures 22 and 23. At the upper left corner of the cavity the pressure is below the reference pressure. The pressure rises along the moving wall, reaching a value greater than the reference pressure near the upper right corner on the last frame. A local minimum exists at the vortex center. The pressure fields for lower Reynolds numbers were similar to those shown in figure 24, but the minimums and maximums along the moving wall were more pronounced.

Figure 25 shows the effect of Reynolds number on the positions of the unsteady vortex centers as well as the terminal positions of the vortex centers for several Reynolds numbers from 100 to 500 in a square cavity. Increasing the Reynolds number shifts the terminal position of the vortex center upstream and farther into the cavity. These positions fall quite close to the asymptote from linear theory (ref. 12), shown as the line drawn from the center of the cavity to the moving wall. The path of the instantaneous vortex centers moves farther downstream before turning down at the wall and then upstream as Reynolds number increases.

Flow visualization. - Numerical flow visualization motion pictures were made for each of the runs. Selected frames from two motion pictures have been chosen to illustrate the numerical flow visualization experiments. Figure 26 is for a square cavity at a Reynolds number of 100. The first frame shows the initial distribution of four particles per cell at the start of the calculation. The remaining frames show that the fluid close to the upper moving surface is dragged along by the upper surface and forced to turn down at the right wall. The fluid flows along the right wall, gradually turning back to the left and then upward, only to be directly influenced by the moving surface and dragged to the right again.

Frames from a positive print of the motion picture of flow in a cavity with an aspect ratio of 2 at a Reynolds number of 100 are given in figure 27. The first frame shows the initial distribution of one particle per cell. Succeeding frames show the development of the flow at dimensionless times of 1, 2, 3, 4, and 10.

The circulatory nature of the flow is evident in these figures, even though it is seen much more dramatically in the motion pictures. The effect of the moving wall can be seen to propagate into the cavity with time. The lower portion of the cavity remains relatively quiescent, even at a dimensionless time of 10. Later frames show the beginnings of the development of the weak vortices. The small triangle above the cavity is used to show the velocity of the moving wall in the motion picture.

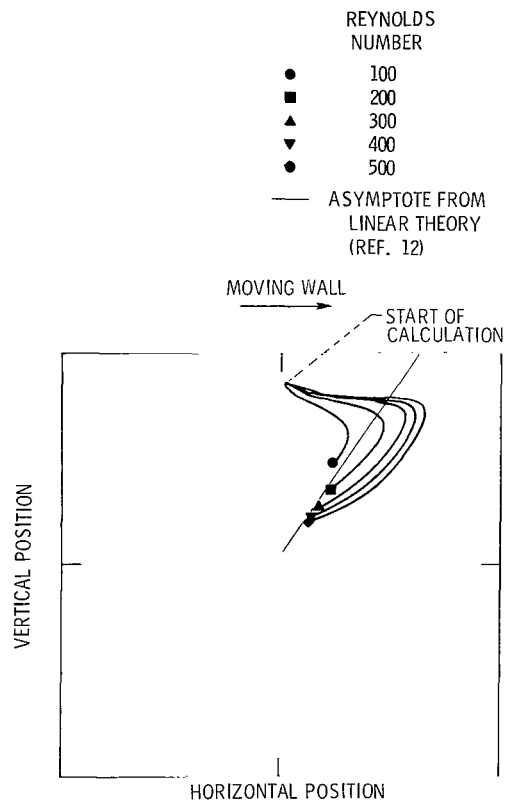
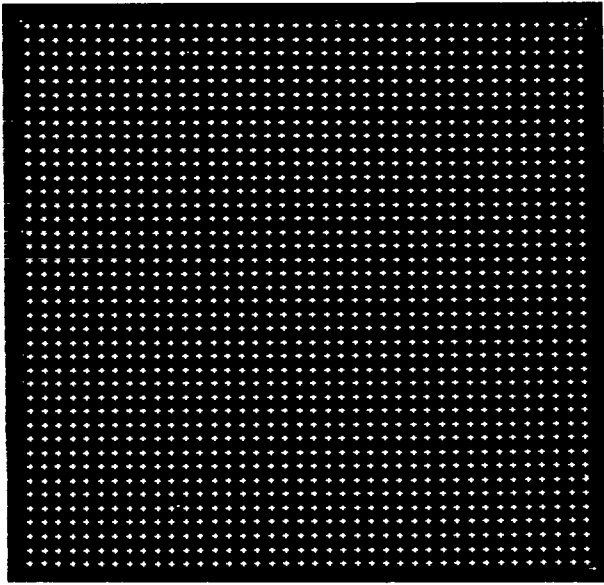
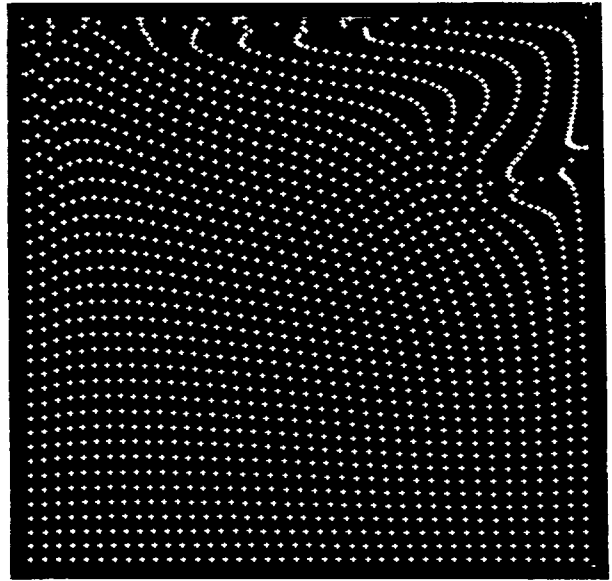


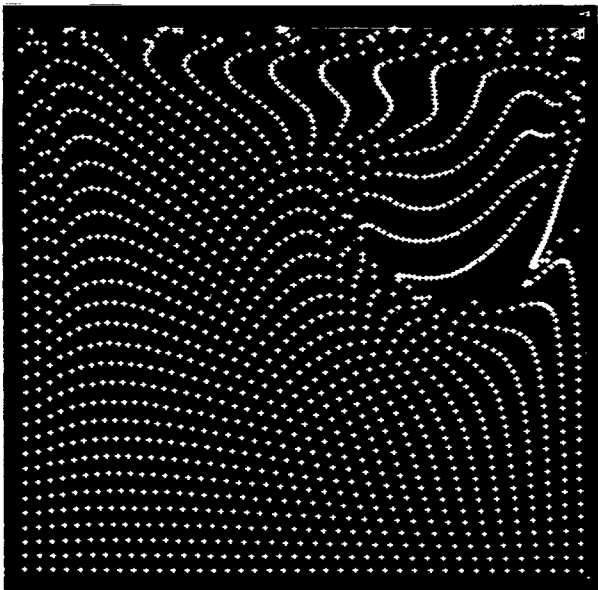
Figure 25, - Path of instantaneous position of vortex centers in square cavity.



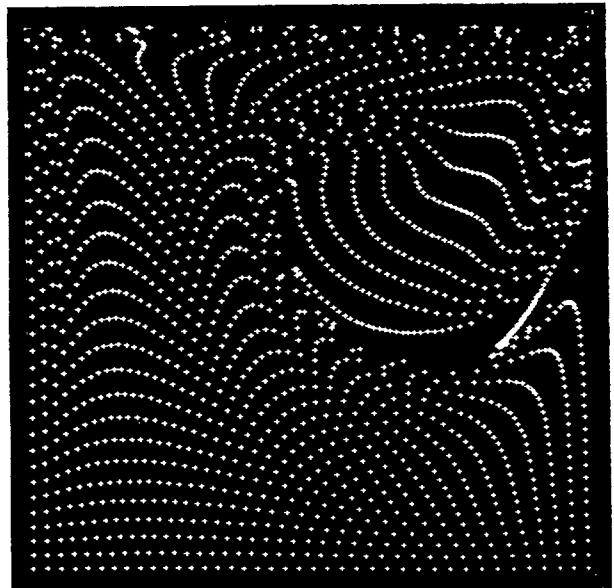
(a) Time, 0.



(b) Time, 1.

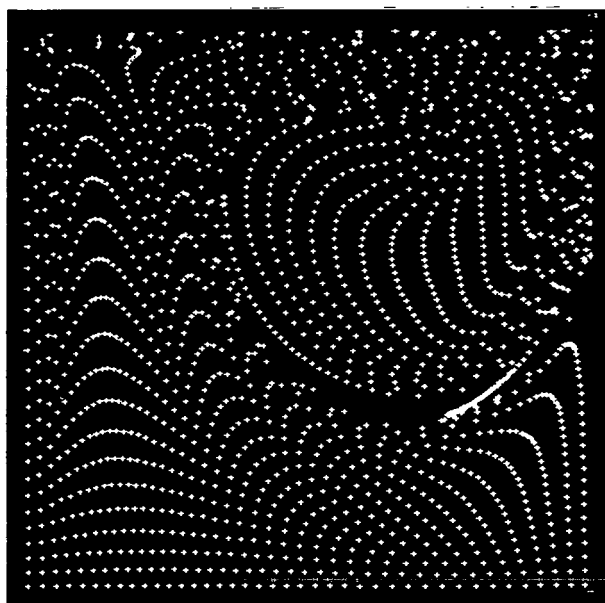


(c) Time, 2.

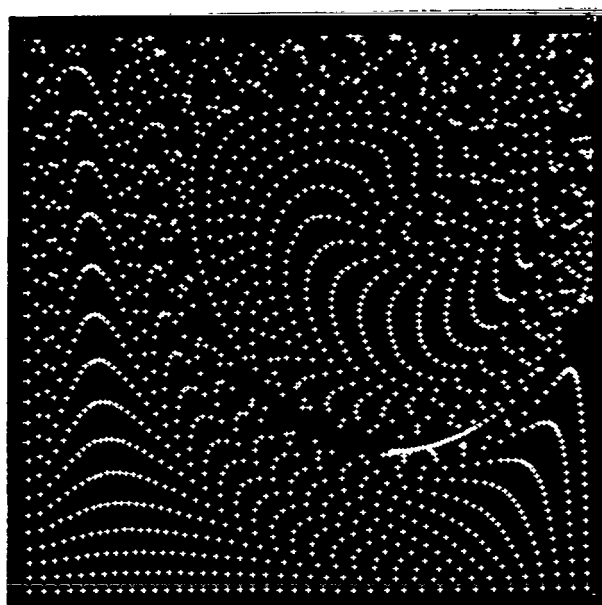


(d) Time, 3.

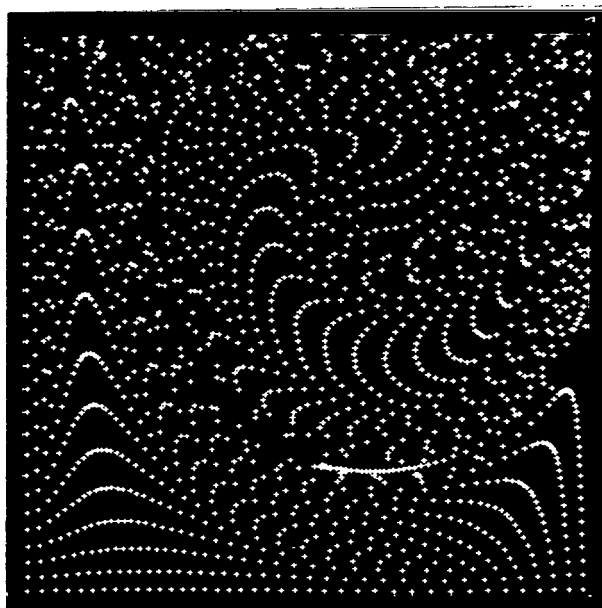
Figure 26. - Numerical flow visualization experiment. Square cavity; Reynolds number, 100. Dimensionless time.



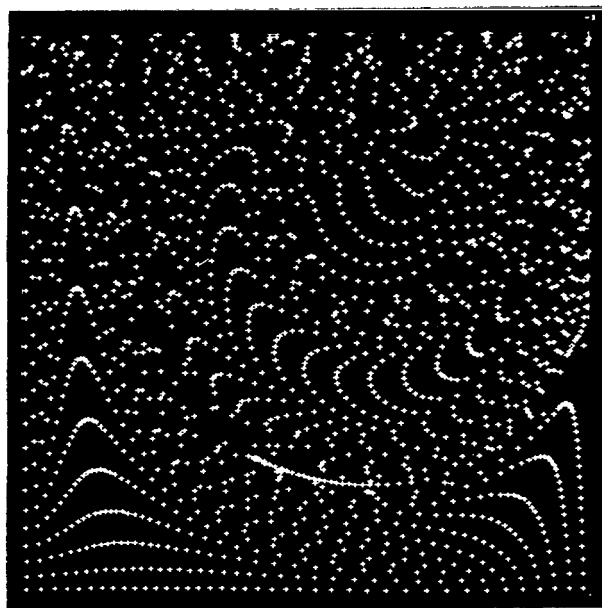
(e) Time, 4.



(f) Time, 5.



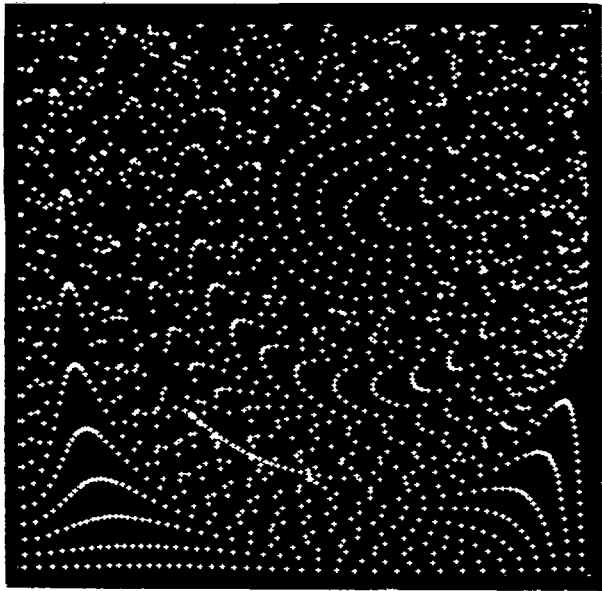
(g) Time, 6.



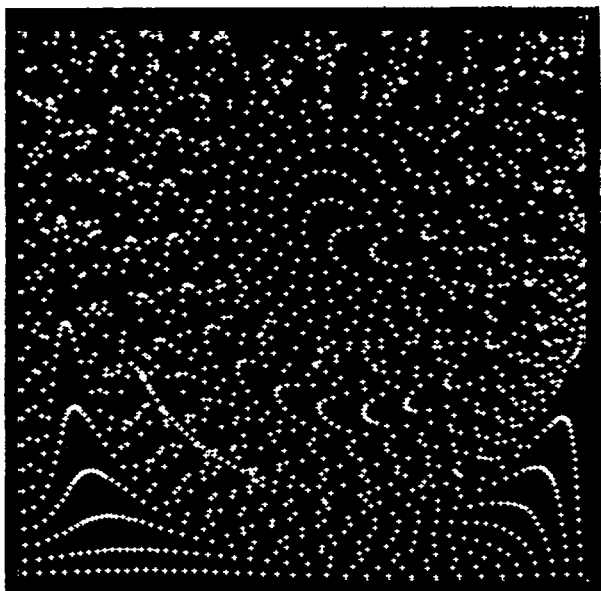
(h) Time, 7.

Figure 26. - Continued.

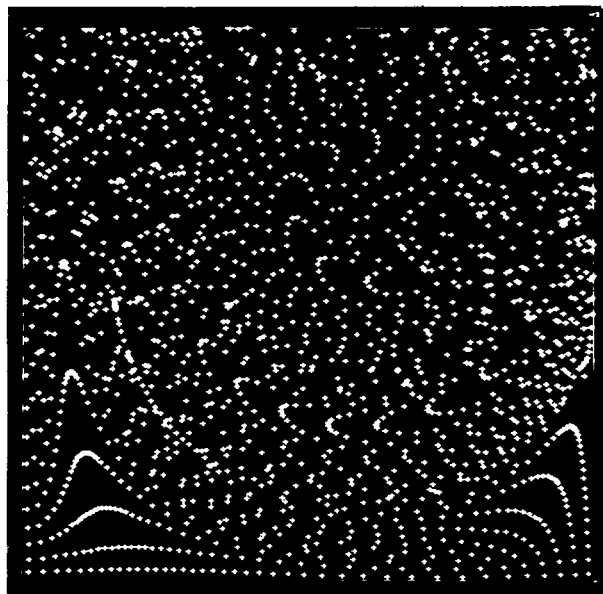




(i) Time, 8.



(j) Time, 9.



(k) Time, 10.

Figure 26. - Concluded.

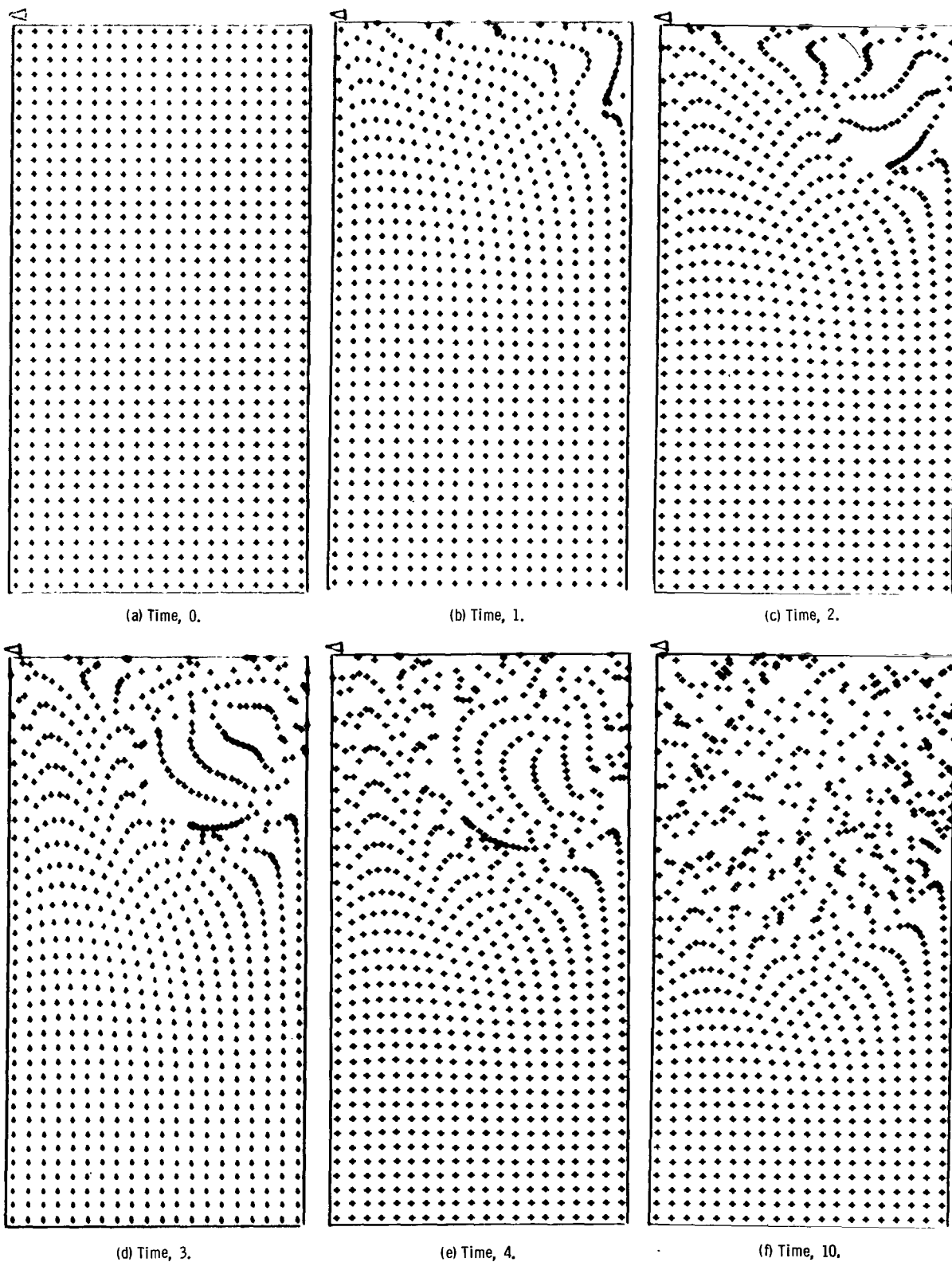


Figure 27. - Numerical flow visualization experiment. Aspect ratio of cavity, 2; Reynolds number, 100. Dimensionless time.

## CONCLUDING REMARKS

A computer program to solve the unsteady, two-dimensional, incompressible Navier-Stokes equations was written. The program was used to investigate unsteady flow in a rectangular cavity with a moving wall. The calculations started with the fluid at rest in the cavity and continued until no further changes in velocity occurred.

Flow in cavities with aspect ratios of  $1/2$  and  $1$  and in the upper part of a cavity with an aspect ratio of  $2$  were similar at a Reynolds number of  $100$ . This was true of the unsteady, as well as the steady, flow.

As the Reynolds number increased from  $100$  to  $500$  in a square cavity the inviscid portion of the flow occupied a progressively larger portion of the cavity. At all these Reynolds numbers the inviscid portion of the flow about the vortex center increased during the initial period.

For a square cavity the path of the instantaneous position of the vortex center approached the downstream wall more closely with increasing Reynolds number, even though the terminal position of the vortex center moved closer to the upstream wall.

No stability problems were encountered in any of the runs. The velocities at large times were compared where possible to velocities calculated from the steady Navier-Stokes equations or the results of steady experiment; generally satisfactory agreement was shown.

A numerical flow visualization experiment was described. This technique uses marked particles to show the motion of the fluid. A microfilm recorder is required in order to display and photograph the particles. At the end of a run the sequence of photographs can be projected as a motion picture which shows clearly the development of the flow. The coding necessary to perform such an experiment is included in the computer program for solving the Navier-Stokes equations.

Lewis Research Center,  
National Aeronautics and Space Administration,  
Cleveland, Ohio, February 1, 1971,  
129-01.

# APPENDIX A

## SYMBOLS

| Mathematical<br>symbol | FORTTRAN<br>symbol | Description  |
|------------------------|--------------------|--|
| d                      | D                  | correction term, eq. (13)                                    |
| $\bar{g}_x, \bar{g}_y$ | -----              | body force in $\bar{x}$ - and $\bar{y}$ -directions          |
| $g_x, g_y$             | GX, GY             | dimensionless body forces, $\bar{L}g/\bar{W}^2$              |
| h                      | H                  | dimensionless cavity length in y-direction                   |
| i                      | I                  | subscript indicating y-position                              |
| j                      | J                  | subscript indicating x-position                              |
| $\bar{L}$              | -----              | reference length (length of moving wall for cavity flow)     |
| n                      | N                  | superscript indicating $n^{\text{th}}$ time step             |
| $\bar{P}$              | -----              | pressure   |
| q                      | -----              | superscript indicating $q^{\text{th}}$ iteration             |
| r                      | R                  | abbreviation, eq. (17)                                       |
| $\bar{t}$              | -----              | time   |
| t                      | T                  | dimensionless time, $\bar{W}t/\bar{L}$                       |
| $\bar{u}$              | -----              | velocity in $\bar{x}$ -direction                             |
| u                      | U                  | dimensionless velocity in x-direction, $\bar{u}/\bar{W}$     |
| $\bar{v}$              | -----              | velocity in $\bar{y}$ -direction                             |
| v                      | V                  | dimensionless velocity in y-direction, $\bar{v}/\bar{W}$     |
| $\bar{W}$              | -----              | reference velocity (velocity of moving wall for cavity flow) |
| w                      | W                  | dimensionless cavity length in x-direction                   |
| $\bar{x}$              | -----              | horizontal direction   |
| x                      | X                  | dimensionless horizontal direction, $\bar{x}/\bar{L}$        |
| $\bar{y}$              | -----              | vertical direction   |
| y                      | Y                  | dimensionless vertical direction, $\bar{y}/\bar{L}$          |
| $\delta t$             | DELT               | time step  |

| Mathematical<br>symbol | FORTTRAN<br>symbol | Description  |
|------------------------|--------------------|--|
| $\delta x$             | DELX               | space increment in x-direction                             |
| $\delta y$             | DELY               | space increment in y-direction                             |
| $\overline{\nu}$       | -----              | fluid kinematic viscosity                                  |
| $\nu$                  | VISC               | dimensionless kinematic viscosity                          |
| $\overline{\rho}$      | -----              | fluid density  |
| $\varphi$              | PHI                | dimensionless pressure, $\overline{P}/\overline{\rho W^2}$ |
| $\omega$               | OMEGA              | relaxation factor  |

## APPENDIX B

### DESCRIPTION OF COMPUTER PROGRAM

The three major calculations performed by the computer program are the solutions of the equations for pressure and for both velocities. Additional calculations are required to determine the position of the vortex center and for particle movement, plotting routines, etc. Since the continuity equation will not be satisfied exactly, the  $d_{i,j}$  will not in general be identically zero. It is necessary, however, that the continuity equation be satisfied sufficiently closely at each time step. Following Harlow (ref. 4), we make sure that each  $d_{i,j}$  is smaller in absolute value than  $3.5 \times 10^{-3}$ .

The Poisson's equation for pressure will be solved iteratively. In order to expedite convergence, successive overrelaxation (see ref. 17) is used. With the introduction of a relaxation factor  $\omega$ , equation (16) becomes

$$\varphi_{i,j}^{q+1} = (1 - \omega)\varphi_{i,j}^q + \omega \frac{1}{2\left(\frac{1}{\delta x^2} + \frac{1}{\delta y^2}\right)} \left( \frac{\varphi_{i,j+1}^q + \varphi_{i,j-1}^q}{\delta x^2} + \frac{\varphi_{i+1,j}^q + \varphi_{i-1,j}^q}{\delta y^2} + r_{i,j} \right) \quad (B1)$$

where the superscript  $q$  indicates the  $q^{\text{th}}$  iteration. The most recently computed values of the  $\varphi$  shown without superscripts are used. A relaxation factor of 1.8 has been used without any attempt at optimization.

The iteration is continued until the field converges to some desired degree. Satisfactory results have been obtained when the criterion suggested by Harlow (ref. 4)

$$\frac{|\varphi_{i,j}^q - \varphi_{i,j}^{q-1}|}{|\varphi_{i,j}^q| + |\varphi_{i,j}^{q-1}| + u_{i,j}^2 + v_{i,j}^2 + |g_x w| + |g_y h|} < 2 \times 10^{-4} \quad (B2)$$

is satisfied at each point.

The velocities are calculated explicitly so that the time step is limited by stability conditions. Hirt (ref. 18) has suggested approximate criteria

$$\nu > \frac{1}{2} \delta t u^2 \quad (B3)$$

and

$$\nu > \frac{1}{2} \delta x^2 \frac{\partial u}{\partial x} \quad (B4)$$

where  $u$  is the average maximum fluid speed and  $\partial u / \partial x$  is the average maximum velocity gradient in the direction of flow. Equation (B3) indicates a time step of 0.02 for a Reynolds number of 100. Equal space increments were used to give a  $20 \times 20$  mesh and it was observed that equation (B4) was satisfied also. The same time and space increments were also found to be satisfactory for Reynolds numbers as large as 500, indicating that these criteria are somewhat conservative for this cavity flow.

It remains to expand terms such as  $u_{i,j}$  prior to coding. Capital letters are used to represent the FORTRAN notation for the finite difference variables. Since fractional subscripts are not allowed,  $U(I,J)$  is used for  $u_{i,j+1/2}$  and  $V(I,J)$  is used for  $v_{i+1/2,j}$ ; the other variables are cell-centered, so that arguments  $(I,J)$  represent  $(i,j)$ .

The computer program was written to be run on an IBM 360 Model 67 computer in the time-sharing mode. Unless the program is being restarted, the BLOCK DATA subprogram named CBLKC must be loaded before the main program named MAIN. Additional routines are required for calculating running time (CPUTIM), microfilm plotting (LRGON, LRCNVT, LRGRID, LRANGE, LRCHSZ, LRLEGN, LRXLEG, LRYLEG, LRTLEG, LRCURV, LRMRGN, LRMON, LRMOFF, LRNON, LRNOFF, LRSON, LRSOFF) given in reference 19, and drawing isometric views (PLOT3D, ROTATE) given in reference 20.

## Outline of Computing Procedure

An outline of MAIN is given below. The names of SUBROUTINE or ENTRY calls are listed at the right.

- |   |              |
|---|--------------|
| (1) Read and write the input data.  | -----        |
| (2) Calculate constants that will be needed.  | INIT, CONSTT |
| (3) Calculate and plot the initial particle positions.                                | PART, PRINTI |
| (4) Calculate D and R at time T.  | DANDR        |
| (5) Calculate PHI at time T + DELT.   | PRESS, ITER  |
| (6) Calculate U and V at time T + DELT.   | UANDV        |
| (7) Calculate the position of the vortex center.                                      | VTXCTR       |
| (8) Calculate and plot the new particle positions.                                    | MOVE         |
| (9) Print D, U, V, and PHI if T = 0, 1, 2, 3, . . .                                   | PRNTN        |
| (10) If T < TLAST, return to step 4; if T = TLAST,<br>prepare final prints and plots. | PRNTF        |

## Input

NAMelist is used for data input; the variables, with default values listed at the right, are any or all of the following:

|            |   |         |
|------------|---|---------|
| DELX, DELY | space increments                                      | 0.05    |
| DELT       | time step   | 0.02    |
| W          | depth/width ratio of cavity                           | 1.0     |
| TLAST      | dimensionless time at which to end calculations       | 2.0     |
| VISC       | kinematic viscosity                                   | 0.01    |
| OMEGA      | relaxation factor                                     | 1.8     |
| MOVIE      | logical variable, true if a motion picture is desired | .FALSE. |
| SECOND     | logical variable, true if program is being restarted  | .FALSE. |
| NPPC       | number of marked particles per cell                   | 1       |

## Output

Marked-particle positions are recorded at every time step in the calculation. Printed output, consisting of all values of D, U, V, and PHI is generated at  $T = 0, 1, 2, 3, \dots$ . At the end of the calculations, microfilm plots are made of the instantaneous positions of the vortex center. Horizontal and vertical velocity traverses through the vortex center and an isometric view of the pressure field are also plotted.

The printed output from the final time for the default values of the input variables is given in appendix C.



# APPENDIX C

## OUTPUT FROM SAMPLE PROBLEM AT DIMENSIONLESS TIME 2

```

-0.2146E-03 -0.1554E-03 -0.7725E-04 -C.1554E-03 -C.4337E-04 -C.4457E-04 -C.4329E-04 -C.1345E-03 -0.2424E-03 -0.1620E-03
-0.1604E-03 -C.2789E-03 -C.9663E-04 -C.2521E-04 -C.7242E-04 -C.0443E-04 -C.1144E-04 -C.0477E-03 -0.7439E-04 -0.4443E-04
-0.7725E-04 -C.1538E-04 -C.0294E-04 -C.5531E-04 -C.6962E-04 -C.1659E-03 -C.0209E-04 -C.1197E-03 -0.2244E-03
-0.6744E-04 -C.7474E-04 -C.4548E-04 -C.1319E-03 -C.1905E-03 -C.9167E-04 -C.8448E-04 -C.1144E-04 -C.9155E-04 -C.1714E-04
-0.9346E-04 -C.2767E-04 -C.1211E-04 -C.1343E-04 -C.1161E-03 -C.8077E-04 -C.0775E-04 -C.1278E-03 -C.2735E-03 -C.4357E-04
-0.3165E-04 -C.2956E-04 -C.1155E-03 -C.1149E-03 -C.1162E-03 -C.1574E-03 -C.1649E-04 -C.2214E-04 -C.9173E-04
-0.2134E-04 -C.5114E-04 -C.1520E-04 -C.0278E-04 -C.3944E-04 -C.1165E-04 -C.1354E-03 -C.1175E-03 -C.2621E-03 -C.9173E-04
-0.1673E-04 -C.2909E-04 -C.0347E-04 -C.0411E-04 -C.1180E-03 -C.5124E-04 -C.6562E-04 -C.2734E-04 -C.1431E-04 -C.2490E-04
-0.1422E-03 -C.5966E-04 -C.4315E-04 -C.1311E-04 -C.1180E-03 -C.5124E-04 -C.3599E-04 -C.2734E-04 -C.2742E-04 -C.3278E-04
-0.4214E-04 -C.7428E-04 -C.2765E-05 -C.4222E-04 -C.2593E-03 -C.1720E-03 -C.5364E-04 -C.1798E-04 -C.2575E-04 -C.9517E-05
-0.3320E-04 -C.3487E-04 -C.1705E-04 -C.7802E-04 -C.1192E-05 -C.8821E-04 -C.1633E-03 -C.8444E-04 -C.9225E-04 -C.1550E-04
-0.4292E-04 -C.2C09E-04 -C.6288E-04 -C.1160E-03 -C.1282E-03 -C.9537E-05 -C.3318E-04 -C.2960E-04 -C.1134E-04 -C.5476E-05
-0.1651E-04 -C.1101E-03 -C.8154E-04 -C.1401E-04 -C.1109E-03 -C.5126E-04 -C.5126E-04 -C.4444E-04 -C.5445E-04 -C.1257E-04
-0.2304E-05 -C.6741E-04 -C.9358E-04 -C.1233E-03 -C.2394E-03 -C.1164E-03 -C.1780E-04 -C.4444E-04 -C.1246E-04 -C.2492E-05
-0.3827E-04 -C.4143E-04 -C.1532E-04 -C.4494E-04 -C.6795E-04 -C.8345E-04 -C.9228E-04 -C.2334E-04 -C.1197E-04
-0.4107E-04 -C.1208E-03 -C.1180E-03 -C.4848E-04 -C.1669E-03 -C.1431E-03 -C.2265E-04 -C.1527E-04 -C.4531E-05
-0.2134E-04 -C.1788E-04 -C.3845E-04 -C.3451E-04 -C.2319E-04 -C.7391E-04 -C.1907E-04 -C.4474E-04 -C.5060E-05 -C.5476E-05
-0.2684E-04 -C.1233E-03 -C.9367E-04 -C.9367E-04 -C.3457E-04 -C.1274E-03 -C.4453E-04 -C.1335E-04 -C.1907E-04 -C.1413E-05
-0.2684E-04 -C.0360E-04 -C.2217E-04 -C.5315E-04 -C.8494E-04 -C.3815E-04 -C.4292E-04 -C.0943E-05 -C.9345E-05 -C.1532E-04
-0.1693E-04 -C.1699E-03 -C.8755E-04 -C.5245E-04 -C.4172E-04 -C.2503E-04 -C.1597E-04 -C.1597E-04 -C.4351E-04 -C.2491E-05
-0.1162E-04 -C.1510E-04 -C.5460E-04 -C.1675E-04 -C.2599E-04 -C.6318E-04 -C.3184E-04 -C.2457E-04 -C.3135E-04 -C.5439E-04
-0.7417E-04 -C.4717E-04 -C.4664E-04 -C.2344E-05 -C.3815E-04 -C.1192E-04 -C.3219E-04 -C.1949E-04 -C.2428E-04 -C.1340E-05
-0.3844E-04 -C.2420E-04 -C.1413E-04 -C.5347E-05 -C.2192E-04 -C.1192E-04 -C.3219E-04 -C.1949E-04 -C.2428E-04 -C.1340E-05
-0.7737E-04 -C.9102E-04 -C.6437E-05 -C.2456E-04 -C.9716E-05 -C.1609E-05 -C.2164E-04 -C.5525E-04 -C.1453E-04
-0.3342E-04 -C.3676E-04 -C.6437E-05 -C.2456E-04 -C.9716E-05 -C.1609E-05 -C.2164E-04 -C.5525E-04 -C.1453E-04
-0.1333E-03 -C.2980E-06 -C.6205E-04 -C.2715E-04 -C.8976E-04 -C.6199E-04 -C.1311E-05 -C.3180E-04 -C.2543E-05
-0.1044E-04 -C.2187E-04 -C.1794E-04 -C.1481E-04 -C.2038E-04 -C.3791E-04 -C.7153E-04 -C.2861E-05 -C.5782E-05 -C.3397E-04
-0.1496E-04 -C.9388E-04 -C.2104E-04 -C.3144E-04 -C.1353E-03 -C.5013E-04 -C.4119E-04 -C.2745E-05 -C.1439E-04 -C.1474E-04
-0.5162E-04 -C.1723E-04 -C.2507E-04 -C.3322E-04 -C.1657E-04 -C.5013E-04 -C.4119E-04 -C.2745E-05 -C.1439E-04 -C.1474E-04
-0.1370E-04 -C.7843E-04 -C.7625E-05 -C.1324E-04 -C.1195E-04 -C.9608E-04 -C.1431E-04 -C.1069E-05 -C.2344E-04 -C.1534E-04
-0.4654E-04 -C.3755E-04 -C.6616E-05 -C.1948E-04 -C.2184E-05 -C.9608E-04 -C.1431E-04 -C.1069E-05 -C.2344E-04 -C.1534E-04
-0.1265E-04 -C.1316E-04 -C.4435E-04 -C.9179E-05 -C.2825E-04 -C.2086E-05 -C.4070E-04 -C.3219E-04 -C.1130E-04 -C.7425E-05
-0.3871E-04 -C.1947E-04 -C.3242E-04 -C.3219E-05 -C.1874E-04 -C.4437E-05 -C.1466E-04 -C.2939E-04 -C.1130E-04 -C.7425E-05
-0.4600E-04 -C.4157E-04 -C.2267E-04 -C.2432E-04 -C.3999E-04 -C.6649E-05 -C.1872E-04 -C.1442E-04 -C.9557E-05 -C.1129E-04
-0.5797E-04 -C.5966E-04 -C.1697E-04 -C.1484E-04 -C.1934E-05 -C.3970E-04 -C.4292E-04 -C.3665E-04 -C.1261E-04 -C.1261E-04
-0.1151E-04 -C.4711E-04 -C.2151E-04 -C.1591E-04 -C.9348E-05 -C.4041E-04 -C.1204E-04 -C.1520E-04 -C.3532E-04 -C.2363E-04
-0.3875E-04 -C.2685E-04 -C.2172E-04 -C.1967E-05 -C.5004E-04 -C.2486E-04 -C.9537E-05 -C.2270E-04 -C.1462E-04 -C.4220E-04
-0.4433E-05 -C.6407E-05 -C.1152E-04 -C.2617E-04 -C.2255E-04 -C.1755E-05 -C.2055E-04 -C.1462E-04 -C.4220E-04
-0.4244E-04 -C.1352E-04 -C.2709E-04 -C.1755E-04 -C.2255E-04 -C.1850E-04 -C.9535E-05 -C.2146E-05 -C.1545E-04 -C.1191E-04
-0.7312E-04 -C.3135E-04 -C.4438E-04 -C.1339E-04 -C.2584E-04 -C.1114E-04 -C.1200E-05 -C.1664E-04 -C.6154E-05 -C.2906E-04

```

```

-0.2215E 00 -0.1711E 10 -0.1219E 00 -0.9109E-01 -C.7172E-01 -C.6846E-01 -C.4850E-01 -C.4045E-01 -C.3364E-01 -C.2771E-01
-0.2249E-01 -0.1786E-01 -C.1377E-01 -C.1316E-01 -C.7013E-02 -C.4350E-02 -C.2226E-02 -C.7254E-03 -C.1251E-04 -C.0
-0.1793E 00 -0.2287E 00 -C.2144E 00 -C.1470E 00 -C.1539E 00 -C.1369E 00 -C.1114E 10 -C.0434E-01 -C.2936E-01 -C.6591E-01
-0.6395E-01 -C.4327E-01 -C.3377E-01 -C.2538E-01 -C.1805E-01 -C.1181E-01 -C.6743E-02 -C.2964E-02 -C.7184E-03 -C.0
-0.1256E 00 -C.2020E 00 -C.2199E 00 -C.2291E 00 -C.1841E 00 -C.1671E 00 -C.1252E 00 -C.1252E 00 -C.1252E 00 -C.8915E-01
-0.7346E-01 -C.5932E-01 -C.4667E-01 -C.3544E-01 -C.2564E-01 -C.1715E-01 -C.1016E-01 -C.4345E-02 -C.1356E-02 -C.0
-0.4242E-01 -C.1635E-01 -C.2035E 10 -C.2161E 10 -C.1941E 10 -C.1797E 00 -C.1596E 00 -C.1394E 00 -C.1104E 00 -C.1007E 00
-0.8338E-01 -C.6763E-01 -C.5346E-01 -C.4196E-01 -C.2979E-01 -C.2022E-01 -C.1224E-01 -C.5981E-02 -C.1734E-02 -C.0
-0.8242E-01 -C.1107E-01 -C.1745E 10 -C.1935E 10 -C.1890E 00 -C.1776E 00 -C.1610E 10 -C.1421E 00 -C.1227E 00 -C.1038E 00
-0.4610E-01 -C.6991E-01 -C.5535E-01 -C.4242E-01 -C.3105E-01 -C.2123E-01 -C.1296E-01 -C.6445E-02 -C.1849E-02 -C.0
-0.4365E-01 -C.1054E 00 -C.1494E 00 -C.1716E 00 -C.1767E 00 -C.1692E 00 -C.1655E 00 -C.1382E 00 -C.1195E 00 -C.1010E 00
-0.8355E-01 -C.6762E-01 -C.5346E-01 -C.4344E-01 -C.3093E-01 -C.2051E-01 -C.1258E-01 -C.6247E-02 -C.1844E-02 -C.0
-0.3349E-01 -C.8632E-01 -C.1288E 00 -C.1532E 00 -C.1613E 00 -C.1576E 00 -C.1461E 00 -C.1304E 00 -C.1120E 00 -C.9398E-01
-0.7702E-01 -C.6175E-01 -C.4836E-01 -C.3578E-01 -C.2684E-01 -C.1837E-01 -C.1128E-01 -C.5623E-02 -C.1665E-02 -C.0
-0.2638E-01 -C.7166E-01 -C.1112E 00 -C.1361E 10 -C.1463E 00 -C.1445E 00 -C.1342E 00 -C.1187E 00 -C.1011E 00 -C.8342E-01
-0.6712E-01 -C.5243E-01 -C.4269E-01 -C.3353E-01 -C.2207E-01 -C.1503E-01 -C.9225E-02 -C.4611E-02 -C.1475E-02 -C.0
-0.2108E-01 -C.5948E-01 -C.9589E-01 -C.1201E 10 -C.1309E 00 -C.1296E 00 -C.1195E 00 -C.1041E 00 -C.8652E-01 -C.6929E-01
-0.6391E-01 -C.4090E-01 -C.3566E-01 -C.2231E-01 -C.1580E-01 -C.1063E-01 -C.6445E-02 -C.3254E-02 -C.9847E-03 -C.0
-0.1671E-01 -C.4953E-01 -C.8142E-01 -C.1336E 10 -C.1133E 00 -C.1115E 00 -C.1008E 00 -C.8445E-01 -C.6747E-01 -C.5101E-01
-0.3706E-01 -C.2613E-01 -C.1804E-01 -C.1225E-01 -C.8143E-02 -C.4292E-02 -C.3193E-02 -C.1653E-02 -C.5072E-03 -C.0
-0.1253E-01 -C.3912E-01 -C.6583E-01 -C.8432E-01 -C.9141E-01 -C.8756E-01 -C.7557E-01 -C.6932E-01 -C.4249E-01 -C.2767E-01
-0.1617E-01 -C.8194E-01 -C.3237E-02 -C.5777E-03 -C.5527E-03 -C.7873E-03 -C.4023E-03 -C.2871E-03 -C.6290E-04 -C.0
-0.7826E-02 -C.2733E-01 -C.4670E-01 -C.5930E-01 -C.6169E-01 -C.5459E-01 -C.4092E-01 -C.2494E-01 -C.1011E-01 -C.1422E-02
-0.8904E-02 -C.1262E-01 -C.1341E-01 -C.1225E-01 -C.9981E-02 -C.7277E-02 -C.4044E-02 -C.3377E-02 -C.2671E-03 -C.0
-0.1867E-02 -C.1138E-01 -C.2112E-01 -C.2482E-01 -C.2614E-01 -C.4575E-02 -C.4575E-02 -C.3745E-01 -C.3046E-01 -C.3623E-01
-0.3755E-01 -C.3547E-01 -C.3097E-01 -C.2536E-01 -C.1940E-01 -C.1366E-01 -C.8514E-02 -C.4279E-02 -C.1273E-02 -C.0
-0.6183E-02 -C.1301E-01 -C.1441E-01 -C.2347E-01 -C.3742E-01 -C.5341E-01 -C.6722E-01 -C.7584E-01 -C.7927E-01 -C.7509E-01
-0.6784E-01 -C.5925E-01 -C.4777E-01 -C.3742E-01 -C.2779E-01 -C.1922E-01 -C.1182E-01 -C.6965E-02 -C.1772E-02 -C.0
-0.1741E-01 -C.4001E-01 -C.6424E-01 -C.8998E-01 -C.1143E 00 -C.1324E 00 -C.1407E 00 -C.1393E 00 -C.1292E 00 -C.1138E 00
-0.9599E-01 -C.7808E-01 -C.6144E-01 -C.4647E-01 -C.3392E-01 -C.2312E-01 -C.1417E-01 -C.9092E-02 -C.2136E-02 -C.0
-0.3804E-01 -C.9332E-01 -C.1344E 00 -C.1792E 00 -C.2106E 00 -C.2242E 00 -C.2199E 00 -C.2015E 00 -C.1749E 00 -C.1450E 00
-0.1163E 00 -C.7073E-01 -C.6907E-01 -C.5117E-01 -C.3651E-01 -C.2455E-01 -C.1491E-01 -C.7454E-02 -C.2219E-02 -C.0
-0.6034E-01 -C.1499E 00 -C.2327E 00 -C.4377E 00 -C.4059E 00 -C.3690E 00 -C.3127E 00 -C.2512E 00 -C.1534E 00 -C.1457E 00
-0.1220E 00 -C.9188E-01 -C.6804E-01 -C.4935E-01 -C.3464E-01 -C.2297E-01 -C.1374E-01 -C.7434E-02 -C.1934E-02 -C.0
-0.1158E 00 -C.2587E 00 -C.3606E 00 -C.4377E 00 -C.4059E 00 -C.3690E 00 -C.3127E 00 -C.2512E 00 -C.1534E 00 -C.1457E 00
-0.1077E 00 -C.7878E-01 -C.5706E-01 -C.4068E-01 -C.2812E-01 -C.1834E-01 -C.1074E-01 -C.6509E-02 -C.1612E-02 -C.0
-0.2433E 00 -C.4057E 00 -C.4684E 00 -C.4589E 00 -C.4056E 00 -C.3330E-01 -C.1937E 00 -C.1937E 00 -C.1414E 00 -C.1019E 00
-0.7308E-01 -C.5229E-01 -C.3727E-01 -C.2620E-01 -C.1762E-01 -C.1134E-01 -C.6346E-02 -C.2745E-02 -C.6179E-03 -C.0
-0.3492E 00 -C.3987E 00 -C.3533E 00 -C.2408E 00 -C.2096E 00 -C.1506E 00 -C.1059E 00 -C.7381E-01 -C.5127E-01 -C.3570E-01
-0.2499E-01 -C.1759E-01 -C.1238E-01 -C.8577E-02 -C.5677E-02 -C.3397E-02 -C.1632E-02 -C.4224E-03 -C.1153E-03 -C.0

```

|             |             |             |             |             |             |             |             |             |             |             |
|-------------|-------------|-------------|-------------|-------------|-------------|-------------|-------------|-------------|-------------|-------------|
| -0.2215F    | 00          | -0.5729F-31 | -0.4692F-01 | -0.3337F-01 | -0.1937F-01 | -0.1337F-01 | -0.0954F-02 | -0.0646F-02 | -0.0481F-02 | -0.5627F-02 |
| -0.5225F-02 | -0.6539F-02 | -0.6096F-02 | -0.3612F-02 | -0.1345F-02 | -0.2655F-02 | -0.2132F-02 | -0.1496F-02 | -0.2374F-03 | -0.2998F-03 | -0.2998F-03 |
| -0.3450F    | 00          | -0.3931F-03 | -0.6755F-01 | -0.6025F-01 | -0.3638F-01 | -0.3921F-01 | -0.2955F-01 | -0.2509F-01 | -0.2145F-01 | -0.1939F-01 |
| -0.3712F-01 | -0.1535F-01 | -0.1361F-01 | -0.1231F-01 | -0.1047F-01 | -0.0962F-02 | -0.7201F-02 | -0.6256F-02 | -0.5312F-02 | -0.7136F-03 | -0.7136F-03 |
| -0.5212F    | 00          | -0.3958F-01 | -0.4969F-01 | -0.7127F-01 | -0.1034F-01 | -0.5819F-01 | -0.5169F-01 | -0.4545F-01 | -0.4663F-01 | -0.3656F-01 |
| -0.3274F-01 | -0.2347F-01 | -0.2629F-01 | -0.2324F-01 | -0.2031F-01 | -0.1735F-01 | -0.1417F-01 | -0.1055F-01 | -0.5534F-02 | -0.2608F-02 | -0.2608F-02 |
| -0.6636F    | 00          | -0.6167E    | 00          | -0.1272F-01 | -0.6543F-01 | -0.7631F-01 | -0.7510F-01 | -0.7074F-01 | -0.4585F-01 | -0.6553F-01 |
| -0.5019F-01 | -0.4529F-01 | -0.4042E-01 | -0.3584F-01 | -0.3139F-01 | -0.2691F-01 | -0.2215F-01 | -0.1684F-01 | -0.1075F-01 | -0.3835F-02 | -0.3835F-02 |
| -0.6624F    | 00          | -0.2335F    | 00          | -0.3103F-01 | -0.4734F-01 | -0.7786F-01 | -0.8650F-01 | -0.8731F-01 | -0.8485F-01 | -0.7975F-01 |
| -0.6770E-01 | -0.6139F-01 | -0.5698F-01 | -0.4377F-01 | -0.4276F-01 | -0.3674F-01 | -0.3042F-01 | -0.2340F-01 | -0.1524F-01 | -0.3646F-02 | -0.3646F-02 |
| -0.7061F    | 00          | -0.2954F    | 00          | -0.7548F-01 | -0.7759F-01 | -0.7344F-01 | -0.9338F-01 | -0.1010F    | -0.1019F    | -0.7284F-01 |
| -0.8534F-01 | -0.7733F-01 | -0.6921F-01 | -0.6131F-01 | -0.5362F-01 | -0.4616F-01 | -0.3935F-01 | -0.2974F-01 | -0.1460F-01 | -0.7529F-02 | -0.7529F-02 |
| -0.3765F    | 00          | -0.3682F    | 00          | -0.1186F    | 00          | -0.326CF-02 | -0.5675F-01 | -0.9707F-01 | -0.1125F    | 00          |
| -0.1023F    | 00          | -0.9259F-01 | -0.8260F-01 | -0.7289F-01 | -0.6363F-01 | -0.5463F-01 | -0.4544F-01 | -0.3539F-01 | -0.2344F-01 | -0.2196F-02 |
| -0.7636F    | 00          | -0.3934F    | 00          | -0.1575F    | 00          | -0.2170F-01 | -0.5509F-01 | -0.9687F-01 | -0.1228F    | 00          |
| -0.1186F    | 00          | -0.1069E    | 00          | -0.9474F-01 | -0.8335F-01 | -0.7209F-01 | -0.6167F-01 | -0.5125F-01 | -0.4001F-01 | -0.2643F-01 |
| -0.7871F    | 00          | -0.4322E    | 00          | -0.1936F    | 00          | -0.4592F-01 | -0.6443F-01 | -0.8121F    | 00          | -0.1488F    |
| -0.1366F    | 00          | -0.1198F    | 00          | -0.1052E    | 00          | -0.9130F-01 | -0.7963F-01 | -0.6684F-01 | -0.5539E-01 | -0.4324F-01 |
| -0.3038F    | 00          | -0.4651F    | 00          | -0.2255F    | 00          | -0.6897F-01 | -0.3463F-01 | -0.1019F    | 00          | -0.1643F    |
| -0.1480F    | 00          | -0.1307E    | 00          | -0.1133F    | 00          | -0.9708F-01 | -0.9267F-01 | -0.6974F-01 | -0.5750F-01 | -0.4482F-01 |
| -0.2416F    | 00          | -0.4917E    | 00          | -0.2522E    | 00          | -0.5658F-01 | -0.2754E-01 | -0.1035E    | 00          | -0.1556F    |
| -0.1555F    | 00          | -0.1387F    | 00          | -0.1182F    | 00          | -0.9974E-01 | -0.8383F-01 | -0.6099F-01 | -0.5731F-01 | -0.4452F-01 |
| -0.3424F    | 00          | -0.5109F    | 00          | -0.2718F    | 00          | -0.9918F-01 | -0.7515E-01 | -0.1130F    | 00          | -0.1692F    |
| -0.1669F    | 00          | -0.1204E    | 00          | -0.1190F    | 00          | -0.9458F-01 | -0.8154E-01 | -0.6272F-01 | -0.5665F-01 | -0.4222F-01 |
| -0.2606F    | 00          | -0.1403F    | 00          | -0.2816F    | 00          | -0.1029F    | 00          | -0.2583F-01 | -0.1839F    | 00          |
| -0.1683F    | 00          | -0.1403F    | 00          | -0.1146F    | 00          | -0.2927F-01 | -0.2958F-01 | -0.6154F-01 | -0.4905F-01 | -0.3748F-01 |
| -0.8199F    | 00          | -0.5146F    | 00          | -0.2772E    | 00          | -0.939CF-01 | -0.4386F-01 | -0.1405E    | 00          | -0.1737F    |
| -0.1810F    | 00          | -0.1307E    | 00          | -0.1041F    | 00          | -0.8261F-01 | -0.5595F-01 | -0.5256F-01 | -0.4216F-01 | -0.3256F-01 |
| -0.8025F    | 00          | -0.4940F    | 00          | -0          |             |             |             |             |             |             |

[illegible]



```

      IF(.NOT.SECOND) T=0.0
C-----CALCULATE THE CONSTANTS NEEDED IN THE VARIOUS SUBROUTINES
      CALL CONST
      IF(SECOND) GO TO 25
      TFIRST=0.0
C-----PRINT IDENTIFYING INFORMATION ABOUT THE RUN AND DESCRIPTIVE
C-----MATERIAL FOR THE MOVIE
      5 CALL INIT
      IF(MOVIE) CALL LEADER
      IF(SECOND) GO TO 6
C-----CALCULATE INITIAL PARTICLE POSITIONS
      CALL PART
C-----PRINT INITIAL PARTICLE POSITIONS
      CALL PRNTI
C-----START OF CALCULATION LOOP
      L=1
      K=2
      TFIRST=DELT
      NFIRST=1
      GO TO 7
      6 TFIRST=T+DELT
      NFIRST=(T+DELT+0.001)/DELT
      7 DO 14 N=NFIRST,NLAST
      T=TFIRST+FLOAT(N-NFIRST)*DELT
C-----CALCULATE D AND R FROM U AND V AT TIME T
      CALL DANDR
C-----CALCULATE PHI AT TIME T+DELT
      CALL PRESS
C-----CALCULATE U AND V AT TIME T+DELT
      CALL UANDV
C-----CALCULATE THE POSITION OF THE VORTEX CENTER
      CALL VTXCTR
C-----MOVE PARTICLES
      CALL MOVE
C-----PRINT NEW PARTICLE POSITIONS
      CALL PRNTN
      8 IF(ABS(T-ACHG).LT.0.001) GO TO 17
      13 GO TO (11,12),L
      11 L= 2
      K= 1
      GO TO 14
      12 L= 1
      K= 2
      14 CONTINUE
      GO TO 9
      17 CALL CPU TIM(N2)
C-----RUNTIM IS CPU TIME IN MINUTES
      RUNTIM=FLOAT(N2-N1)/1000000.0
      WRITE(6,15) T
      WRITE(6,28) RUNTIM
      WRITE(6,23) ((D(I,J),I=3,JJ),J=3,JJ)
      WRITE(6,18) ((U(I,J,K),J=3,JJ),I=3,II)
      WRITE(6,19) ((V(I,J,K),J=3,JJ),I=3,II)
      WRITE(6,20) ((PHI(I,J),J=2,JJP1),I=2,IIP1)
      WRITE(6,26)
      BACKSPACE 6
      ACHG=ACHG+A
      WRITE(10) T,U,V,PHI,D,L,K,DCON,PCON,MAXIT,ITER0,ITER1, -

```

```

1 MLAST,MMAX,X,Y,ACHG,VERTPS,VPROFL,HORZPS,UPROFL,VCX,VCY
REWIND 10
IF( T.LT.TLAST ) GO TO 13
9 IF(MOVIE) CALL TAIL
WRITE(10) T,U,V,PHI,D,L,K,DCON,PCON,MAXIT,ITERO,ITERI,
1 MLAST,MMAX,X,Y,ACHG,VERTPS,VPROFL,HORZPS,UPROFL,VCX,VCY
REWIND 10
C-----PRINT FINAL FRAME OF MOVIE AND POSITIONS OF VORTEX CENTERS
CALL PRNTE
STOP
25 WRITE(6,15) T
WRITE(6,23) ((D(I,J),J=3,JJ),I=3,II)
WRITE(6,18) ((U(I,J,K),J=3,JJ),I=3,II)
WRITE(6,19) ((V(I,J,K),J=3,JJ),I=3,II)
WRITE(6,20) ((PHI(I,J),J=2,JJP1),I=2,IIP1)
WRITE(6,26)
BACKSPACE 6
GO TO 5
15 FORMAT(4HIT= ,F10.4)
16 FORMAT(1H0,10(F6.3))
18 FORMAT(2H1U/(10E12.4))
19 FORMAT (2H1V/(10E12.4))
20 FORMAT (4H1PHI/(11E11.4))
23 FORMAT(2H0D/(10E12.4))
26 FORMAT(1X,'JOB TERMINATED HERE')
28 FORMAT(12HOCPU TIME = ,E16.8,7HMINUTES)
END

```

```

FUNCTION FPRESS(X,Y)
COMMON DELX,DELY,DELT,W,H,TLAST,VISC,OMEGA,GX,GY,
1 DELXSQ,DELYSQ,DX4,DY4,GXDELX,GYDELY,VISCX,VISCY,COMOG,OMGOZ,
2 XOY,XOYS,VX,VY,VXY,FDELX,FDELY,TDXDY,DXODY,DYODX,GYHGXB,NLAST,
3 K,L,II,JJ,IIP1,JJP1,IIM1,JJM1,N,T,DELPHI,DMAX,CONMAX,XMAX,NPART
COMMON/UVP/U(44,44,2),V(44,44,2),PHI(44,44),D(44,44),R(44,44),
1 DCON,PCON,MAXIT,ITERO,ITERI,SOMAX
I=Y
J=X
FPRESS=50.0*PHI(I,J)
RETURN
END

```

```

SUBROUTINE CONSTT
C-----CALCULATES CONSTANTS
COMMON DELX,DELY,DELT,W,H,TLAST,VISC,OMEGA,GX,GY,
1 DELXSQ,DELYSQ,DX4,DY4,GXDELX,GYDELY,VISCX,VISCY,COMOG,OMGOZ,
2 XOY,XOYS,VX,VY,VXY,FDELX,FDELY,TDXDY,DXODY,DYODX,GYHGXB,NLAST,
3 K,L,II,JJ,IIP1,JJP1,IIM1,JJM1,N,T,DELPHI,DMAX,CONMAX,XMAX,NPART
COMMON/UVP/U(44,44,2),V(44,44,2),PHI(44,44),D(44,44),R(44,44),
1 DCON,PCON,MAXIT,ITERO,ITERI,SOMAX
GX=0.0

```

```

      GY=0.0
      DELXSQ=DELX**2
      DELYSQ=DELY**2
      DX4=4.0*DELXSQ
      DY4=4.0*DELYSQ
      GXDELX=GX*DELX
      GYDELY=GY*DELY
      VISCX=2.0*VISC/DELX
      VISCY=2.0*VISC/DELY
C-----OMEGA IS THE RELAXATION FACTOR
      COMOG= 1.0 - OMEGA
      OMOGZ=OMEGA/(2.0*(1.0/DELXSQ+1.0/DELYSQ))
      XOY=DELX/(2.0*DELY)
      XOYS=VISC*DELX/DELYSQ
      VY=VISC/DELYSQ
      VX=VISC/DELXSQ
      VXY=VISC/(DELX*DELY)
      FDELX=4.0*DELX
      FDELY=4.0*DELY
      TDXY=2.0*DELX*DELY
      DXOY=DELX/DELY
      DYODX= DELY/DELX
      GYHGXW=ABS(GY*H)+ABS(GX*W)
      NLAST=(TLAST+0.001)/DELT
      II= 2.0 + H/DELY
      JJ= 2.0 + W/DELX
      IIP1=II+1
      IIM1=II-1
      JJP1=JJ+1
      JJM1=JJ-1
      RETURN
      END

```

```

      SUBROUTINE INIT
C-----PRINTS IDENTIFYING INFORMATION
      INTEGER BBBR(8)
      EXTERNAL FPRESS
      LOGICAL CUBE
      COMMON DELX,DELY,DELT,W,H,TLAST,VISC,OMEGA,GX,GY,
1 DELXSQ,DELYSQ,DX4,DY4,GXDELX,GYDELY,VISCX,VISCY,COMOG,OMOGZ,
2 XOY,XOYS,VX,VY,VXY,FDELX,FDELY,TDXY,DXOY,DYODX,GYHGXW,NLAST,
3 K,L,II,JJ,IIP1,JJP1,IIM1,JJM1,N,T,DELPHI,DMAX,CONMAX,XMAX,NPART
      COMMON/UVP/U(44,44,2),V(44,44,2),PHI(44,44),D(44,44),R(44,44),
1 DCON,PCON,MAXIT,ITERO,ITERI,SDMAX
      COMMON/MI/M,MLAST,X(1600),Y(1600)
      COMMON/VC/VCX(1500),VCY(1500),JCH(50),NPPC
      COMMON/LABEL/LAB(15)
      COMMON/PL/VPROFL(50),UPROFL(50),VERTPS(50),HORZPS(50)
      DIMENSION LABA(15)
      DIMENSION S(3800)
      DIMENSION CHART(3)
      DIMENSION FIN(6)
      DIMENSION VXC(16)
      DIMENSION BX(5),BY(5)
      DIMENSION DE(5),CE(6),IC(3),IK(3)

```

```

DIMENSION INT1(7),INT2(20),INT3(18),INT4(14),UNX(2),UNY(2)
DIMENSION TITL1(39)
DIMENSION FRAMX(8),FRAMY(8)
DIMENSION XVEL(11),YPOS(5),TPAR(12),YVEL(12),XPOS(5),TPND(13)
DIMENSION VCXP(1600),VCYP(1600)
CURE =.FALSE.
DATA LABA/4H PRE,4HSSUR,4HE. ,4HWALL,4H MCV,4HES I,4HN Y ,4HDIRE,
14HCTIO,4HN. /
DATA FRAMX/1.0,9.0,1.0,9.0,1.0,1.0,9.0,9.0/
DATA FRAMY/8.066,8.066,1.934,1.934,1.934,8.066,1.934,8.066/
DATA VXC/'POSITION OF VORTEX CENTER$C1UPPER WALL MOVES FROM LEFT T
10 RIGHT'/
DATA FIN/'$C9$D4$R9$R9$R6THE END'/
DATA SYMBOL/'+'/'
DATA WL/'3'/
DATA CHARX/'X'/
DATA CHARY/'Y'/
DATA CHART(1)/' T= '/
DATA BX(1),BX(4),BX(5)/3*2.5/,BY(1),BY(2),BY(5)/3*2.5/
DATA XW/2.0/,YW/2.5/
DATA DE/'SDMAX = '/,CE/' CONMAX = '/
DATA IO/'ITER0 = '/,IK/'ITERI = '/
DATA INT1/'$D3$R9$R9$R4$S$INPUT DATA'/
DATA INT2/'$D5$R7$GND$GFX = $LOXXXXXXXX$R6$GND$GFY = $R1XXXXXXXX$R6 -
1$GND$GFT = $L3'/
DATA INT3/'$D7$R7R$WNE$WF = 1/VISCOSITY = $L6 $R4OMEGA = -
1 $L6'/
DATA INT4/'$D9$R7G$WNX$WF = $L5XXXX$R6G$WNY$WF = $L7'/
DATA TITL1/'$C4$R9$R9$R9A$D3$L8COMPUTER SOLUTION$D3$L9$L2OF THE$C3
1$R9$R3UNSTEADY NAVIER-STOKES EQUATIONS$D3$L9$L9$L2FOR FLOW$D3$L6IN
2 A$D3$L9$L4TWO DIMENSIONAL CAVITY'/
DATA UNX/22.0,32.0/,UNY/48.0,48.0/
DATA SVCU/'H'/
DATA XVEL/'VELOCITY COMPONENT PARALLEL TO MOVING WALL'/
DATA YPOS/'VERTICAL POSITION'/
DATA TPAP/'VERTICAL VELOCITY TRAVERSE THROUGH VORTEX CENTER'/
DATA YVEL/'VELOCITY COMPONENT PERPENDICULAR TO MOVING WALL'/
DATA XPOS/'HORIZONTAL POSITION'/
DATA TPND/'HORIZONTAL VELOCITY TRAVERSE THROUGH VORTEX CENTER'/
DATA BBBB/5*' ', ' LEO', ' DON', 'OVAN'/
VPROFL(1)=1.0
HORZPS(1)=0.0
VERTPS(1)=W
DO 1 I=1,15
1 LAB(I)=LABA(I)
IRF=1.0/VISC
IIM2=II-2
JJM2=JJ-2
FIIM2=IIM2
FJJM2=JJM2
FII=II
FJJ=JJ
XRNG=JJ+3
YRNG=II+3
IF(W-H) 6,7,8
6 XMRG=3.5
YMRG=2.0
GO TO 9

```

```

7 XMRG=2.0
  YMRG=2.0
  GO TO 9
8 XMRG=2.0
  YMRG=3.5
9 BX(2)=FLOAT(JJ)+0.5
  BX(3)=BX(2)
  BY(3)=FLOAT(II)+0.5
  BY(4)=BY(3)
C-----PRINTS IDENTIFYING INFORMATION
C-----
  CALL LRCON
  CALL LRCNV(DELX,3,INT2(6),3,8,2)
  CALL LRCNV(DELY,3,INT2(12),3,8,2)
  CALL LRCNV(DELT,3,INT2(19),3,5,2)
  CALL LRCNV(IRE,1,INT3(9),1,8,0)
  CALL LRCNV(OMEGA,3,INT3(17),3,5,2)
  CALL LRCNV(GX,3,INT4(7),3,4,2)
  CALL LRCNV(GY,3,INT4(14),3,4,2)
  CALL LRGRID(1,1,0.0,0.0)
  CALL LRANGE(0.0,55.0,0.0,55.0)
  CALL LRLEGN(INT1,25,0,1.0,9.6,0.0)
  CALL LRCURV(UNX,UNY,2,2,SYM,0.0)
  CALL LRLEGN(INT2,90,0,1.0,9.6,0.0)
  CALL LRLEGN(INT3,72,0,1.0,9.6,0.0)
  CALL LRLEGN(INT4,56,0,1.0,9.6,1.0)
  CALL LRLEGN(TITL1,153,0,1.0,9.6,1.0)
  RETURN
  ENTRY LEADER
  CALL LRCON
  CALL LRMRGN(0.0,0.0,0.0,0.0)
  CALL LRANGE(0.0,10.0,0.0,10.0)
  CALL LRGRID(1,1,0.0,0.0)
  CALL LRCON
  DO 20 I=1,32
20 CALL LRCURV(X,Y,0,1,SYM,1.0)
  EOP=0.0
  DO 21 I=1,5
  IF(I.EQ.5) EOP=1.0
  CALL LRCURV(FRAMEX,FRAMY,4,2,SYM,0.0)
21 CALL LRCURV(FRAMEX(5),FRAMY(5),4,2,SYM,EOP)
  DO 22 I=1,48
22 CALL LRCURV(X,Y,0,1,SYM,1.0)
  EOP=0.0
  DO 23 I=1,5
  IF(I.EQ.5) EOP=1.0
  CALL LRCURV(FRAMEX,FRAMY,4,2,SYM,0.0)
23 CALL LRCURV(FRAMEX(5),FRAMY(5),4,2,SYM,EOP)
  DO 24 I=1,5
24 CALL LRCURV(X,Y,0,1,SYM,1.0)
  CALL LRMOFF
  RETURN
  ENTRY PRNTI
C-----PRINTS INITIAL PARTICLE POSITIONS
C-----
  CALL LRMRGN(XMRG,XMRG,YMRG,YMRG)
  CALL LRANGE(0.0,XRNG,0.0,YRNG)
  CALL LRGRID(1,1,0.0,0.0)
  CALL LRXLFG(CHARX,1)

```



```

CALL LRYLEG(CHARY,1)
CALL LRCNVT(T,3,CHART(2),3,8,2)
CALL LRTLFG(CHART,12)
CALL LRCURV(BX,BY,5,2,SYM,0.0)
CALL LRNON
CALL LRCURV(X,Y,Mlast,5,SYMBOL,1.0)
CALL LRNOFF
RETURN
ENTRY PRNTN
C-----PRINTS NEW PARTICLE POSITIONS
C-----
CALL LRMRGN(XMRG,XMRG,YMRG,YMRG)
CALL LRANGE(C.0,XRNG,C.0,YRNG)
CALL LRGRID(1,1,0.0,0.0)
YW=YW + DELT/DELY
IF( YW.GE.FLOAT(II)+0.49) YW=2.5
CALL LRCNVT(T,3,CHART(2),3,8,2)
CALL LRCNVT(SDMAX,3,DE(3),4,9,2)
CALL LRLEGN(DE,17,0,3.0,10.0,C.0)
CALL LRCNVT(CONMAX,3,CE(4),4,9,2)
CALL LRLEGN(CE,21,0,5.6,10.0,C.0)
CALL LRCNVT(ITER0,1,IO(3),1,4,0)
CALL LRLEGN(IO,12,0,3.5,0.4,0.0)
CALL LRCNVT(ITER1,1,IK(3),1,4,0)
CALL LRLEGN(IK,12,0,6.1,0.4,0.0)
CALL LRXLEG(CHARX,1)
CALL LRYLEG(CHARY,1)
CALL LRTLFG(CHART,12)
C-----POSITION OF MARKER INDICATING VELOCITY OF WALL
CALL LRCURV(XW,YW,1,4,WL,0.0)
C-----OUTLINE OF CAVITY
CALL LRCURV(BX,BY,5,2,SYM,0.0)
CALL LRNON
CALL LRSON
CALL LRCURV(X,Y,Mlast,5,SYMBOL,1.0)
CALL LRSOFF
CALL LRNOFF
RETURN
ENTRY TAIL
DO 25 I=1,48
25 CALL LRCURV(X,Y,0,1,SYM,1.0)
RETURN
ENTRY PRNTE
C-----PRINTS FINAL FRAME OF MOVIE AND POSITIONS OF VORTEX CENTERS
C-----
CALL LRMON
CALL LRLEGN(FIN,22,C,1.0,9.6,1.1)
C-----NORMALIZE THE VORTEX CENTER POSITIONS
DO 2 I=1,NLAST
VCXP(I)=W*(1.0-(VCX(I)-2.5)/FJJM2)
2 VCYP(I)=(VCY(I)-2.5)/FIIM2
VCXN=VCXP(NLAST)
VCYN=VCYP(NLAST)
CALL LRANGE(0.0,H,0.0,W)
CALL LRGRID(2,2,0.5,0.5)
CALL LRMRGN(YMRG,YMRG,XMRG,XMRG)
CALL LRCHSZ(3)
CALL LRTLFG(VXC,63)

```

```

C-----POSITION OF UNSTEADY VORTEX CENTER AT END OF CALCULATION
      CALL LRCURV(VCYN,VCXN,1,4,SVCU,0.0)
C-----POSITION OF UNSTEADY VORTEX CENTER DURING CALCULATIONS
      CALL LRCHSZ(0)
      CALL LRCURV(VCYP,VCXP,NLAST,2,SYM,1.0)
      CALL LRGRID(2,2,0.25,0.25)
      IVC = VCYN(NLAST) + 0.5
      JVC = VCXN(NLAST) + 0.5
      PL = 0.5 + VCYN(NLAST) - FLOAT(IVC)
      QL = 0.5 + VCXN(NLAST) - FLOAT(JVC)
C-----TRAVERSE PERPENDICULAR TO MOVING WALL
      DO 4 JJP=3,JJ
        JP = JJP - 1
        VPROFL(JP) = PL*V(IVC,JJP,K) + (1.0-PL)*V(IVC-1,JJP,K)
4      VERTPS(JP)=W*(1.0-(FLOAT(JJP)-2.5)/FJJM2)
        CALL LRMRGN(1.0,0.4,1.0,0.4)
        CALL LRANGE(-0.5,1.0,0.0,W)
        CALL LRXLEG(XVEL,42)
        CALL LRYLEG(YPOS,17)
        CALL LRTLEG(TPAR,43)
        CALL LRCURV(VPROFL(2),VERTPS(2),JJM2,4,SVCU,0.0)
        CALL LRCURV(VPROFL,VERTPS,JJ,2,SC,1.0)
C-----TRAVERSE PARALLEL TO MOVING WALL
      DO 5 IIP=3,II
        IP = IIP - 1
        UPROFL(IP) = -QL*U(IIP,JVC,K) - (1.0-QL)*U(IIP,JVC-1,K)
5      HORZPS(IP)=( FLOAT(IIP)-2.5 )/FIIM2
        CALL LRANGE(0.0,H,-0.5,1.0)
        CALL LRXLEG(XPOS,19)
        CALL LRYLEG(YVEL,47)
        CALL LRTLEG(TPND,50)
        CALL LRCURV(HORZPS(2),UPROFL(2),IIM2,4,SVCU,0.0)
        CALL LRCURV(HORZPS,UPROFL,II,2,SC,1.0)
C-----3D PRESSURE PLOT
      IF(W.GT.H) JJM2=JJM2/2
      IF(W.LT.H) IIM2=IIM2/2
      CALL PLOT3D(3.0,FJJ,3.0,FII,S,IIM2,JJM2,IIM2,JJM2,FPRESS,CUBE)
      CALL ROTATE(0.0,0.0,45.0,.TRUE.,.FALSE.)
      CALL ROTATE(0.0,35.0,0.0,.TRUE.,.FALSE.)
      RETURN
      END
      CALL LRMON
      SUBROUTINE DANDR
C-----CALCULATES DISCREPANCY AND SOURCE TERM FOR POISSON'S EQUATION
      COMMON DELX,DELY,DELT,W,H,TLAST,VISC,OMEGA,GX,GY,
1      DELXSQ,DELYSQ,DX4,DY4,GXDELX,GYDELY,VISCX,VISCY,COMOG,OMG07,
2      XOY,XOYS,VX,VY,VXY,FDELX,FDELY,TDXDY,DXDDY,DYDDX,GYHGXY,NLAST,
3      K,L,II,JJ,IIP1,JJP1,IIM1,JJM1,N,T,DELPHI,DMAX,CONMAX,XMAX,NPART
      COMMON/UVPU(44,44,2),V(44,44,2),PHI(44,44),D(44,44),R(44,44),
1      DCON,PCON,MAXIT,ITER0,ITERI,SDMAX
      DMAX= 0.0
      DO 22 J=3,JJ
        DO 22 I=3,II
          D(I,J)= (U(I,J,L)-U(I,J-1,L)) / DELX+(V(I,J,L)-V(I-1,J,L)) / DELY
          IF (ABS(D(I,J)).LE.DMAX) GO TO 22
          DMAX=ABS(D(I,J))
          SDMAX=D(I,J)
        22
      22

```

C-----GENERAL TERM

```

22 R(I,J)= ((U(I,J+1,L)+U(I,J,L))*2 - 2.0*(U(I,J,L)+U(I,J-1,L))*2
1 + (U(I,J-1,L)+U(I,J-2,L))*2)/DX4
2 + ((V(I+1,J,L)+V(I,J,L))*2 - 2.0*(V(I,J,L)+V(I-1,J,L))*2
3 + (V(I-1,J,L)+V(I-2,J,L))*2)/DY4
4 + ((U(I+1,J,L)+U(I,J,L))*(V(I,J+1,L)+V(I,J,L))
5 + (U(I,J-1,L)+U(I-1,J-1,L))*(V(I-1,J,L)+V(I-1,J-1,L))
6 - (U(I,J,L)+U(I-1,J,L))*(V(I-1,J+1,L)+V(I-1,J,L))
7 - (U(I+1,J-1,L)+U(I,J-1,L))*(V(I,J,L)+V(I,J-1,L)))/TDXDY
8 - D(I,J)/DELT
27 DO 23 J=3, JJ

```

C-----ROW ABOVE UPPER WALL

```

R(2,J)= 0.25*( DYDDX*( (U(3,J,L)+U(2,J,L))*(V(2,J+1,L)+V(2,J,L))
1 - (U(3,J-1,L)+U(2,J-1,L))*(V(2,J,L)+V(2,J-1,L)))
2 + ( (V(3,J,L)+V(2,J,L))*2-(V(2,J,L)+V(1,J,L))*2 )
3 - 0.5*VISCX*( DYDDX*(V(2,J+1,L)-2.0*V(2,J,L)+V(2,J-1,L))
4 - (U(3,J,L)-U(3,J-1,L)-U(2,J,L)+U(2,J-1,L))) -GYDELY

```

C-----ROW BELOW LOWER WALL

```

23 R(II+1,J)= -0.25*(( (V(II+1,J,L)+V(II,J,L))*2
1 - (V(II,J,L)+V(II-1,J,L))*2)
2 + DYDDX*( (U(II+1,J,L)+U(II,J,L))*(V(II,J+1,L)+V(II,J,L))
3 - (U(II+1,J-1,L)+U(II,J-1,L))*(V(II,J,L)+V(II,J-1,L)))
4 + 0.5*VISCX*( DYDDX*(V(II,J+1,L)-2.0*V(II,J,L)+V(II,J-1,L))
5 - (U(II+1,J,L)-U(II+1,J-1,L)-U(II,J,L)+U(II,J-1,L))) + GYDELY
DO 24 I=3, II

```

C-----COLUMN BEFORE LEFT WALL

```

R(I,2)= 0.25*(( (U(I,3,L)+U(I,2,L))*2 - (U(I,2,L)+U(I,1,L))*2)
1 + DXDDY*( (U(I+1,2,L)+U(I,2,L))*(V(I,3,L)+V(I,2,L))
2 - (U(I-1,2,L)+U(I,2,L))*(V(I-1,3,L)+V(I-1,2,L)))
3 - 0.5*VISCY*( DXDDY*( U(I+1,2,L)-2.0*U(I,2,L)+U(I-1,2,L) )
4 - (V(I,3,L)-V(I-1,3,L)-V(I,2,L)+V(I-1,2,L))) -GXDELX

```

C-----COLUMN AFTER RIGHT WALL

```

24 R(I,JJ+1)= -0.25*(( (U(I,JJ+1,L)+U(I,JJ,L))*2
1 - (U(I,JJ,L)+U(I,JJ-1,L))*2 )
2 + DXDDY*( (U(I+1,JJ,L)+U(I,JJ,L))*(V(I,JJ+1,L)+V(I,JJ,L))
3 - (U(I-1,JJ,L)+U(I,JJ,L))*(V(I-1,JJ+1,L)+V(I-1,JJ,L)))
4 + 0.5*VISCY*( DXDDY*( U(I+1,JJ,L)-2.0*U(I,JJ,L)+U(I-1,JJ,L))
5 - (V(I,JJ+1,L)-V(I-1,JJ+1,L)-V(I,JJ,L)+V(I-1,JJ,L)))
6 + GXDELX
RETURN
END

```

SUBROUTINE PRESS

C-----CONTROLS ITERATION OF POISSON'S EQUATION AND DETERMINES CONVERGENCE

```

COMMON DELX,DELY,DELT,W,H,TLAST,VISC,OMEGA,GX,GY,
1 DELXSQ,DELYSQ,DX4,DY4,GXDELX,GYDELY,VISCX,VISCY,COMOG,OMGOZ,
2 XOY,XOYS,VX,VY,VXY,FDELX,FDELY,TDXDY,DXDDY,DYDDX,GYHGXY,NLAST,
3 K,L,II,JJ,IIP1,JJP1,IIM1,JJM1,N,T,DELPHI,DMAX,CONMAX,XMAX,NPART
COMMON/UVPU(44,44,2),V(44,44,2),PHI(44,44),D(44,44),R(44,44),
1 DCON,PCCN,MAXIT,ITERO,ITERI,SDMAX
DIMENSION CON(44,44),TEST(44,44),CONST(44,44)
IL = 2 + (II-2)/2
DO 36 J=2,JJP1
DO 36 I=2,IIP1

```

```

36 CONST(I,J)= 0.25*((U(I,J,L)+U(I,J-1,L))*2
1 + (V(I,J,L)+V(I-1,J,L))*2)+GYHGXW
IF( ITERO.NE.1 ) GO TO 31
IF( ITERI.EQ.5 ) GO TO 31
ITERI = ITERI - 1
31 DO 35 IQUT=1,MAXIT
C-----MAXIT IS MAXIMUM NUMBER OF ITERATIONS
ITERO = IQUT
DO 32 IIN=1,ITERI
CALL ITER
32 CONTINUE
DO 33 J=2,JJP1
DO 33 I=2,IIP1
33 TEST(I,J)= PHI(I,J)
CALL ITER
CONMAX=0.0
C-----TEST FOR CONVERGENCE
DO 34 J=3,JJ
DO 34 I=3,II
CON(I,J)=ABS( PHI(I,J)-TEST(I,J) )/(ABS( PHI(I,J) )
1 + ABS( TEST(I,J) ) + CONST(I,J) )
IF( CON(I,J).GT.CONMAX ) CONMAX=CON(I,J)
34 CONTINUE
IF( CONMAX.LE.PCON ) GO TO 37
35 CONTINUE
ITERO = MAXIT
RETURN
37 TST = 0.25*( PHI(IL,JJ)+PHI(IL,JJP1)+PHI(IL+1,JJ)+PHI(IL+1,JJP1) )
CHG = 1.0-TST
C-----NORMALIZE TO PHI= 1.0 AT CENTER OF WALL OPPOSITE MOVING WALL
DO 38 J=2,JJP1
DO 38 I=2,IIP1
PHI(I,J) = PHI(I,J) + CHG
38 CONTINUE
RETURN
END

```

```

SUBROUTINE ITER
COMMON DELX,DELY,DELT,W,H,TLAST,VISC,OMEGA,GX,GY,
1 DELXSQ,DELYSQ,DX4,DY4,GXDELX,GYDELY,VISCX,VISCY,COMOG,OMGOZ,
2 XOY,XOYS,VX,VY,VXY,FDELX,FDELY,TDXDY,DXDDY,DYDDX,GYHGXW,TLAST,
3 K,L,II,JJ,IIP1,JJP1,IIM1,JJM1,N,T,DELPHI,DMAX,CONMAX,XMAX,NPART
COMMON/UVP/U(44,44,2),V(44,44,2),PHI(44,44),D(44,44),R(44,44),
1 DCON,PCON,MAXIT,ITERO,ITERI,SDMAX
C-----ROW ABOVE UPPER WALL
DO 41 J=3,JJ
41 PHI(2,J)= PHI(3,J)+R(2,J)
C-----COLUMN BEFORE LEFT WALL
DO 43 I=3,II
PHI(I,2)= PHI(I,3)+R(I,2)
DO 42 J=3,JJ
C-----GENERAL TERM
42 PHI(I,J)= COMOG*PHI(I,J)+OMGC7*((PHI(I,J+1)+PHI(I,J-1))/DELXSQ
1 + (PHI(I+1,J)+PHI(I-1,J))/DELYSQ+R(I,J))

```

```

C-----COLUMN AFTER RIGHT WALL
  43 PHI(I,JJ+1)= PHI(I,JJ)+R(I,JJ+1)
C-----ROW BELOW LOWER WALL
  DO 44 J=3,JJ
    44 PHI(II+1,J)= PHI(II,J) + R(II+1,J)
    RETURN
  END

SUBROUTINE UANDV
C-----CALCULATES AXIAL AND NORMAL VELOCITIES
  COMMON DELX,DELY,DELT,W,H,TLAST,VISC,OMEGA,GX,GY,
  1 DELXSQ,DELYSQ,DX4,DY4,GXDELX,GYDELY,VISCX,VISCY,COMOG,OMGOZ,
  2 XOY,XOYS,VX,VY,VXY,FDELX,FDELY,TDXDY,DXODY,DYODX,GYHGXB,NLAST,
  3 K,L,II,JJ,IIP1,JJP1,IIM1,JJM1,N,T,DELPHI,DMAX,CONMAX,XMAX,NPART
  COMMON/UVP/U(44,44,2),V(44,44,2),PHI(44,44),D(44,44),R(44,44),
  1 DCON,PCON,MAXIT,ITERO,ITERI,SDMAX
  DO 52 I=3,II
    DO 52 J=3,JJ
C-----GENERAL TERMS
      U(I,J,K)= U(I,J,L)+DELT*(((U(I,J,L)+U(I,J-1,L))*2
      1 - (U(I,J+1,L)+U(I,J,L))*2)/FDELX
      2 + ((U(I,J,L)+U(I-1,J,L))*(V(I-1,J+1,L)+V(I-1,J,L))
      3 - (U(I+1,J,L)+U(I,J,L))*(V(I,J+1,L)+V(I,J,L)))/FDFLY
      4 + GX+(PHI(I,J)-PHI(I,J+1))/DELX
      5 + VY*(U(I+1,J,L)-2.0*U(I,J,L)+U(I-1,J,L))
      6 - VXY*(V(I,J+1,L)-V(I-1,J+1,L)-V(I,J,L)+V(I-1,J,L)))
      V(I,J,K)= V(I,J,L)+DELT*(((U(I+1,J-1,L)+U(I,J-1,L))
      1 *(V(I,J,L)+V(I,J-1,L))-(U(I+1,J,L)+U(I,J,L))
      2 *(V(I,J+1,L)+V(I,J,L)))/FDELX
      3 + ((V(I,J,L)+V(I-1,J,L))*2-(V(I+1,J,L)+V(I,J,L))*2)/FDELY
      4 + GY+(PHI(I,J)-PHI(I+1,J))/DELY
      5 + VX*(V(I,J+1,L)-2.0*V(I,J,L)+V(I,J-1,L))
      6 - VXY*(U(I+1,J,L)-U(I,J,L)-U(I+1,J-1,L)+U(I,J-1,L)))
    52 CONTINUE
    DO 53 J=3,JJ
C-----LOWER NO SLIP ROW
      53 V(II,J,K)= 0.0
C-----RIGHT NO SLIP WALL
    DO 51 I=3,II
      51 U(I,JJ,K)= 0.0
C-----CALCULATE BOUNDARY VALUES
    DO 54 J=3,JJM1
C-----ROW ABOVE UPPER NO SLIP WALL
      U(2,J,K)= -U(3,J,K)
      V(1,J,K)= -V(3,J,K)
C-----ROW BELOW LOWER NO SLIP WALL
      U(II+1,J,K)= -U(II,J,K)
      54 V(II+1,J,K)= -V(II-1,J,K)
      V(1,JJ,K)= -V(3,JJ,K)
      V(II+1,JJ,K)= -V(II-1,JJ,K)
    DO 55 I=3,IIM1
C-----COLUMN BEFORE LEFT MOVING NO SLIP WALL
      U(I,1,K)= -U(I,3,K)
      V(I,2,K)= 2.0-V(I,3,K)

```

C-----COLUMN AFTER RIGHT NO SLIP WALL

U(I,JJ+1,K) = -U(I,JJ-1,K)

55 V(I,JJ+1,K) = -V(I,JJ,K)

U(II,1,K) = -U(II,3,K)

U(II,JJ+1,K) = -U(II,JJ-1,K)

C-----UPPER LEFT CORNER

U(2,2,K) = U(3,2,K)

V(2,2,K) = V(2,3,K)

C-----LOWER LEFT CORNER

U(II+1,2,K) = U(II,2,K)

C V(II,2,K) = V(II,3,K)

C-----UPPER RIGHT CORNER

U(2,JJ,K) = -U(3,JJ,K)

V(2,JJ+1,K) = V(2,JJ,K)

C-----LOWER RIGHT CORNER

U(II+1,JJ,K) = -U(II,JJ,K)

V(II,JJ+1,K) = V(II,JJ,K)

RETURN

END

SUBROUTINE VTXCTR

C-----CALCULATES THE POSITION OF THE VORTEX CENTER

COMMON DELX,DELY,DFLT,W,H,TLAST,VISC,OMEGA,GX,GY,

1 DELXSQ,DELYSQ,DX4,DY4,GXDELX,GYDELY,VISCX,VISCY,COMOG,OMGOZ,

2 X0Y,X0YS,VX,VY,VXY,FDELX,FDELY,TDXDY,DXODY,DYODX,GYHGXB,NLAST,

3 K,L,II,JJ,IIP1,JJP1,IIM1,JJM1,N,T,DELPHI,DMAX,CONMAX,XMAX,NPART

COMMON/UVP/U(44,44,2),V(44,44,2),PHI(44,44),D(44,44),R(44,44),

1 DCON,PCON,MAXIT,ITER0,ITERI,SDMAX

COMMON/VC/VCX(1500),VCY(1500),JCH(50),NPPC

FUNCT(A,B)=ABS( A/(A-B) )

DO 93 I=3,IIM1

DO 91 J=3,JJM1

IF (V(I,J,K)\*V(I,J+1,K).LE.0.C) GO TO 92

91 CONTINUE

VCX(N) = 0.0

VCY(N) = 0.0

RETURN

92 JCH(I) = J

93 CONTINUE

JCH(II) = JCH(IIM1)

DO 94 I=12,IIM1

IHOLD = I

J0 = JCH(I-1)

J1 = JCH(I)

J2 = JCH(I+1)

IF( U(I,J1,K)\*U(I+1,J2,K).LE.0.C ) GO TO 95

94 CONTINUE

VCX(N) = 0.0

VCY(N) = 0.0

RETURN

95 IF( ABS(U(IHOLD+1,J2,K)).GT.ABS(U(IHOLD,J1,K)) ) GO TO 96

C-----UPPER HALF CELL

X1= FLOAT(J1)+FUNCT( V(IHOLD,J1,K),V(IHOLD,J1+1,K) )

X2= FLOAT(J2)+FUNCT( V(IHOLD+1,J2,K),V(IHOLD+1,J2+1,K) )

```

      Y1 = FLOAT(IHOLD)+0.5
      GO TO 97
C-----LOWER HALF CELL
      96 X1= FLOAT(J0)+FUNCT( V(IHOLD-1,J0,K),V(IHOLD-1,J0+1,K) )
        X2= FLOAT(J1)+FUNCT( V(IHOLD,J1,K),V(IHOLD,J1+1,K) )
        Y1 = FLOAT(IHOLD)-0.5
      97 IF( J2.NE.J1 ) GO TO 103
        IF( ABS(V(IHOLD,J1+1,K)).GE.ABS(V(IHOLD,J1,K)) ) GO TO 100
C-----LEFT HALF CELL
      DO 98 I=11,IIM1
        IM=I
        IF( U(I+1,J1+1,K)*U(I,J1+1,K).LE.0.0 ) GO TO 99
      98 CONTINUE
        VCX(N)=0.0
        VCY(N)=0.0
        RETURN
      99 Y3= FLOAT(IHOLD)+FUNCT( U(IHOLD,J1,K),U(IHOLD+1,J1,K) )
        Y4= FLOAT(IM)+FUNCT( U(IM,J1+1,K),U(IM+1,J1+1,K) )
        X3 = FLOAT(J1) + 0.5
        GO TO 108
C-----RIGHT HALF CELL
      100 DO 101 I=11,IIM1
        IM= I
        IF( U(I,J1-1,K)*U(I+1,J1-1,K).LE.0.0 ) GO TO 102
      101 CONTINUE
        VCX(N)= 0.0
        VCY(N)= 0.0
        RETURN
      102 Y3= FLOAT(IM)+FUNCT( U(IM,J1-1,K),U(IM+1,J1-1,K) )
        Y4= FLOAT(IHOLD)+FUNCT( U(IHOLD,J1,K),U(IHOLD+1,J1,K) )
        X3 = FLOAT(J1) - 0.5
        GO TO 108
C-----J2.NE.J1
      103 DO 104 I=IHOLD,IIM1
        IM1 = I
        IF( U(I,J1,K)*U(I+1,J1,K).LE.0.0 ) GO TO 109
      104 CONTINUE
        VCX(N) = 0.0
        VCY(N) = 0.0
        RETURN
      109 DO 105 I=11,IIM1
        IM2 = I
        IF( U(I,J2,K)*U(I+1,J2,K).LE.0.0 ) GO TO 106
      105 CONTINUE
        VCX(N) = 0.0
        VCY(N) = 0.0
        RETURN
      106 IF( J2.GT.J1 ) GO TO 107
        Y3= FLOAT(IM2)+FUNCT( U(IM2,J2,K),U(IM2+1,J2,K) )
        Y4= FLOAT(IM1)+FUNCT( U(IM1,J1,K),U(IM1+1,J1,K) )
        X3 = FLOAT(J2) + 0.5
        GO TO 108
      107 Y3= FLOAT(IM1)+FUNCT( U(IM1,J1,K),U(IM1+1,J1,K) )
        Y4= FLOAT(IM2)+FUNCT( U(IM2,J2,K),U(IM2+1,J2,K) )
        X3 = FLOAT(J1) + 0.5
      108 RS = (Y3-Y1+(Y4-Y3)*(X1-X3))/(1.0-(Y4-Y3)*(X2-X1))
        VCY(N) = Y1 + RS

```

```

VCX(N) = X1 + (X2-X1)*RS
RETURN
END

```

```

SUBROUTINE PART
C-----GENERATES INITIAL PARTICLE DISTRIBUTION
COMMON DELX,DELY,DELT,W,H,TLAST,VISC,OMEGA,GX,GY,
1 DELXSQ,DELYSQ,DX4,DY4,GXDELX,GYDELY,VISCX,VISCY,COMOG,OMGOZ,
2 XOY,XOYS,VX,VY,VXY,FDELX,FDELY,TDXOY,DXODY,DYODX,GYHGXW,NLAST,
3 K,L,II,JJ,IIP1,JJP1,IIM1,JJM1,N,T,DELPHI,DMAX,CONMAX,XMAX,NPART
COMMON/UEP/U(44,44,2),V(44,44,2),PHI(44,44),D(44,44),R(44,44),
1 DCON,PCON,MAXIT,ITERO,ITERI,SDMAX
COMMON/MI/M,MLAST,X(1600),Y(1600)
COMMON/VC/VCX(1500),VCY(1500),JCH(50),NPPC
IIM2T=2*(II-2)
M=0
IF(NPPC.EQ.4) GO TO 62
C-----ONE PARTICLE PER CELL ( DELX=DELY )
DO 61 J=3,JJ
XJ=J
DO 61 I=3,II
YI=I
M=M+1
X(M)=XJ
61 Y(M)=YI
MLAST=M
RETURN
C-----FOUR PARTICLES PER CELL ( DELX=DELY )
62 DO 64 J=3,JJ
XJ=FLOAT(J)-0.25
DO 63 I=3,II
YI=FLOAT(I)-0.25
M=M+1
X(M)=XJ
Y(M)=YI
X(M+IIM2T)=XJ+0.5
Y(M+IIM2T)=YI
M=M+1
X(M)=XJ
Y(M)=YI+0.5
X(M+IIM2T)=XJ+0.5
63 Y(M+IIM2T)=YI+0.5
M=M+IIM2T
64 CONTINUE
MLAST=M
RETURN
END

```



```

SUBROUTINE MOVE
C-----CALCULATES PARTICLE MOVEMENT
COMMON DELX,DELY,DELT,W,H,TLAST,VISC,OMEGA,GX,GY,
1 DELXSQ,DELYSQ,DX4,DY4,GXDELX,GYDELY,VISCX,VISCY,COMOG,OMG07,
2 XOY,XOYS,VX,VY,VXY,FDELX,FDELY,TDXDY,DXDDY,DYCDX,GYHGXB,NLAST,
3 K,L,II,JJ,IIP1,JJP1,IIM1,JJM1,N,T,DELPHI,DMAX,CNMAX,XMAX,NPART
COMMON/UEP/U(44,44,2),V(44,44,2),PHI(44,44),D(44,44),R(44,44),
1 DCON,PCON,MAXIT,ITER0,ITER1,SDMAX
COMMON/MI/M,MLAST,X(1600),Y(1600)
F(A,B,C,D) = (1.0-P)*(1.0-Q)*A + P*(1.0-Q)*B + Q*(1.0-P)*C + P*Q*D
DO 75 M=1,MLAST
C-----PARTICLE IS IN I,J CELL
I = Y(M) + 0.5
J = X(M) + 0.5
C-----FRACTIONAL PARTS OF PARTICLE POSITIONS
FRACY= Y(M) - FLOAT(I)
FRACX= X(M) - FLOAT(J)
P= FRACX + 0.5
IF( FRACY.GE.0.0 ) GO TO 71
C-----UPPER HALF CELL
Q = -FRACY
IF( I.EQ.3 ) GO TO 76
UM = F( U(I,J-1,K),U(I,J,K),U(I-1,J-1,K),U(I-1,J,K) )
GO TO 72
C-----LOWER HALF CELL
71 Q = 1.0 - FRACY
IF( I.EQ.II ) GO TO 77
UM = F( U(I+1,J-1,K),U(I+1,J,K),U(I,J-1,K),U(I,J,K) )
72 Q = 0.5 - FRACY
IF( FRACX.GE.0.0 ) GO TO 73
C-----LEFT HALF CELL
P = 1.0 + FRACX
IF( J.EQ.3 ) GO TO 78
VM = F( V(I,J-1,K),V(I,J,K),V(I-1,J-1,K),V(I-1,J,K) )
GO TO 74
C-----RIGHT HALF CELL
73 P = FRACX
IF( J.EQ.JJ ) GO TO 79
VM = F( V(I,J,K),V(I,J+1,K),V(I-1,J,K),V(I-1,J+1,K) )
74 X(M) = X(M) + UM*DELT/DELX
Y(M) = Y(M) + VM*DELT/DELY
75 CONTINUE
RETURN
76 UM = (1.0-P)*U(3,J-1,K) + P*U(3,J,K)
GO TO 72
77 UM = (1.0-P)*U(II,J-1,K) + P*U(II,J,K)
GO TO 72
78 VM = (1.0-Q)*V(I,3,K) + Q*V(I-1,3,K)
GO TO 74
79 VM = (1.0-Q)*V(I,JJ,K) + Q*V(I-1,JJ,K)
GO TO 74
END

```

```

      BLOCK DATA
C-----SETS INITIAL CONDITIONS
      COMMON/ UVP/ U(44,44,2), V(44,44,2), PHI(44,44), D(44,44), R(44,44),
1 DCON, PCON, MAXIT, ITER0, ITERI, SDMAX
      COMMON/ PL/ VPROFL(50), UPROFL(50), VERTPS(50), HORIZPS(50)
      DATA U/3872*0.0/, V/45*0.0, 41*2.0, 1895*0.0, 41*2.0, 1850*0.0/
      DATA PHI/1936*1.0/
      DATA DCON/3.5E-3/, PCON/2.0E-4/, MAXIT/100/
      DATA ITER0/100/, ITERI/15/
      DATA VERTPS/50*0.0/, VPROFL/50*0.0/, HORIZPS/50*1.0/, -
1 UPROFL/50*0.0/
      END

```

## REFERENCES

1. Ames, W. F.: Nonlinear Partial Differential Equations in Engineering, Academic Press, 1965.
2. Fromm, Jacob E.; and Harlow, Francis H.: Numerical Solution of the Problem of Vortex Street Development. *Phys. Fluids*, vol. 6, no. 7, July 1963, pp. 975-982.
3. Pearson, Carl E.: Numerical Solutions for the Time-Dependent Viscous Flow Between Two Rotating Coaxial Disks. *J. Fluid Mech.*, vol. 21, pt. 4, Apr. 1965, pp. 623-633.
4. Welch, J. E.; Harlow, F. H.; Shannon, J. P.; and Daly, B. J.: The MAC Method - A Computing Technique for Solving Viscous, Incompressible, Transient Fluid-Flow Problems Involving Free Surfaces. Rep. LA-3425, Los Alamos Scientific Lab., Mar. 21, 1966.
5. Donovan, Leo F.: A Numerical Solution of Unsteady Flow in a Two-Dimensional Square Cavity. *AIAA J.*, vol. 8, no. 3, Mar. 1970, pp. 524-529.
6. Rosenhead, Louis, ed.: *Laminar Boundary Layers*. Clarendon Press, 1963.
7. Hirt, C. W.; and Harlow, Francis H.: A General Corrective Procedure for the Numerical Solution of Initial-Value Problems. *J. Computational Phys.*, vol. 2, no. 2, Nov. 1967, pp. 114-119.
8. Mills, Ronald D.: Numerical Solutions of the Viscous Flow Equations for a Class of Closed Flows. *J. Roy. Aeron. Soc.*, vol. 69, no. 658, Oct. 1965, pp. 714-718.
9. Pan, Frank; and Acrivos, Andreas: Steady Flows in Rectangular Cavities. *J. Fluid Mech.*, vol. 28, pt. 4, June 22, 1967, pp. 643-655.
10. Kawaguti, Mitutosi: Numerical Solution of the Navier-Stokes Equations for the Flow in a Two-Dimensional Cavity. *J. Phys. Soc. Japan*, vol. 16, no. 12, Nov. 1961, pp. 2307-2315.
11. Weiss, Robert F.; and Florsheim, Bruce H.: Flow in a Cavity at Low Reynolds Number. *Phys. Fluids*, vol. 8, no. 9, Sept. 1965, pp. 1631-1635.
12. Burggraf, Odus R.: Analytical and Numerical Studies of the Structure of Steady Separated Flows. *J. Fluid Mech.*, vol. 24, pt. 1, Jan. 1966, pp. 113-151.
13. Runchal, A. K.; Spalding, D. B.; and Wolfshtein, M.: The Numerical Solution of the Elliptic Equations for Transport of Vorticity, Heat and Matter in Two-Dimensional Flows. Rep. SF/TN/2, Imperial College of Science and Technology, London, Aug. 1967.

14. Greenspan, D.: Numerical Studies of Prototype Cavity Flow Problems. Computer J., vol. 12, Feb. 1969, pp. 88-93.
15. Zuk, J.; and Renkel, H. E.: Numerical Solutions for the Flow and Pressure Fields in an Idealized Spiral Grooved Pumping Seal. Proceedings of the Fourth International Conference on Fluid Sealing. Special Publ. 2, ASLE, 1969.
16. Greenspan, D.; Jain, P. C.; Manohar, R.; Noble, B.; and Sakurai, A.: Work in Progress at the Mathematics Research Center on the Numerical Solution of the Navier-Stokes Equations. Proceedings of the ARO Working Group on Computers. Rep. AROD-65-1, Army Research Office, Feb. 1965, pp. 213-260. (Available from DDC as AD-613592.)
17. Varga, Richard S.: Matrix Iterative Analysis. Prentice-Hall, Inc., 1962.
18. Hirt, C. W.: Heuristic Stability Theory for Finite-Difference Equations. J. Computational Phys., vol. 2, no. 4, June 1968, pp. 339-355.
19. Kannenberg, Robert G.: CINEMATIC-FORTRAN Subprograms for Automatic Computer Microfilm Plotting. NASA TM X-1866, 1969.
20. Canright, R. Bruce, Jr.; and Swigert, Paul: PLOT3D - A Package of FORTRAN Subprograms to Draw Three-Dimensional Surfaces. NASA TM X-1598, 1968.

Lewis Motion Picture (C-271) is available on loan. Requests will be filled in the order received.

This tutorial motion picture "Computer-Generated Flow Visualization Motion Pictures" (12 min, color, sound) shows how a computer solution of the equations of fluid motion can be presented as a calculated flow visualization experiment. A motion picture of the flow is made by using special particles that are moved with the fluid, displayed on a cathode ray tube, and photographed with a motion picture camera.

Lewis Motion Picture C-271 is available on request to:

Chief, Management Services Division (5-5)  
National Aeronautics and Space Administration  
Lewis Research Center  
21000 Brookpark Road  
Cleveland, Ohio 44135

CUT

Date

Please send, on loan, copy of Lewis Film C-271.

Name of Organization

Street Number

City and State

Zip Code

NATIONAL AERONAUTICS AND SPACE ADMINISTRATION

WASHINGTON, D. C. 20546

OFFICIAL BUSINESS  
PENALTY FOR PRIVATE USE \$300

FIRST CLASS MAIL



POSTAGE AND FEES PAID  
NATIONAL AERONAUTICS AND  
SPACE ADMINISTRATION

07U 001 33 51 3DS 71.10 00903  
AIR FORCE WEAPONS LABORATORY /WLOL/  
KIRTLAND AFB, NEW MEXICO 87117

ATT E. LOU BOWMAN, CHIEF, TECH. LIBRARY

POSTMASTER: If Undeliverable (Section 158  
Postal Manual) Do Not Return

*"The aeronautical and space activities of the United States shall be conducted so as to contribute . . . to the expansion of human knowledge of phenomena in the atmosphere and space. The Administration shall provide for the widest practicable and appropriate dissemination of information concerning its activities and the results thereof."*

— NATIONAL AERONAUTICS AND SPACE ACT OF 1958

## NASA SCIENTIFIC AND TECHNICAL PUBLICATIONS

**TECHNICAL REPORTS:** Scientific and technical information considered important, complete, and a lasting contribution to existing knowledge.

**TECHNICAL NOTES:** Information less broad in scope but nevertheless of importance as a contribution to existing knowledge.

**TECHNICAL MEMORANDUMS:** Information receiving limited distribution because of preliminary data, security classification, or other reasons.

**CONTRACTOR REPORTS:** Scientific and technical information generated under a NASA contract or grant and considered an important contribution to existing knowledge.

**TECHNICAL TRANSLATIONS:** Information published in a foreign language considered to merit NASA distribution in English.

**SPECIAL PUBLICATIONS:** Information derived from or of value to NASA activities. Publications include conference proceedings, monographs, data compilations, handbooks, sourcebooks, and special bibliographies.

**TECHNOLOGY UTILIZATION PUBLICATIONS:** Information on technology used by NASA that may be of particular interest in commercial and other non-aerospace applications. Publications include Tech Briefs, Technology Utilization Reports and Technology Surveys.

*Details on the availability of these publications may be obtained from:*

SCIENTIFIC AND TECHNICAL INFORMATION OFFICE  
NATIONAL AERONAUTICS AND SPACE ADMINISTRATION  
Washington, D.C. 20546